

One-pot synthesis and characterisation of alkyl functionalised silicon nanoparticles, using an inverse micelle based method.

Jason Thomas

School of Chemistry
University of East Anglia
Norwich
UK
2014

A thesis submitted in fulfilment of the requirements for the degree of
Master of Science by Research of the University of East Anglia.

© This copy of the thesis has been supplied on condition that anyone who consults it is understood to recognise that its copyright rests with the author and that use of any information derived there from must be in accordance with current UK Copyright Law. In addition, any quotation or extract must include full attribution.

Declaration

I declare that the work contained in this thesis submitted for the degree of Master of Science by Research is my work, except where due reference is made to other authors, and has not previously been submitted by me for a degree at this or any other university.

Jason Thomas

Acknowledgments

Firstly, I would like to thank my supervisor Dr Yimin Chao principally for his constant support and constructive criticism throughout my research project, and also for provision of facilities, chemicals and equipment.

Thanks also to Dr Francesca Baldelli-Bombelli, my secondary supervisor, for her support and discussion.

I would also take this opportunity to thank all past and present members of the Chao group whom I have had the pleasure of working with: Mr Shane Ashby, Dr Jayshree Ahire, Miss Ruoxi Liu, Mr Wenchao Zhang, Miss Mehrnaz Behray, Dr Paul Coxon, Dr Qi Wang and Mr Frederik Huld for their insights and friendship.

I would also like to express deep gratitude to my family and close friends for their encouragement and support.

Abstract

Silicon nanoparticles (SiNPs) are subject to research in a variety of fields and their synthesis is of increasing importance. A simple, cheap and easily scalable solution based synthesis method of alkyl terminated SiNPs is reported here. The produced SiNPs were imaged with a transmission electron microscope and have a spherical silicon core approximately 5 nm in diameter. The particles also show a strong blue photoluminescence (PL) emission at 420 nm; demonstrating a stability of luminescence over long periods of time.

Further study of these particles indicated the presence of alkoxy impurities in the surface chemistry. This was caused by the introduction of alcohol to the system in order to quench the lithium aluminium hydride (LiAlH_4) reducing agent. Because of this problem a further refined synthesis approach is reported, whereby suitable modification and optimisation of the reaction mechanism encourages more desirable surface capping, and a much lower surface oxide level. This is accomplished by the introduction of anhydrous copper (II) chloride (CuCl_2) as an alternative to alcohol. However, this approach greatly increased the amount of solid by-product from the reaction and thus complexity of purification, resulting in a decreased overall yield.

The optical properties of SiNPs are of particular interest, since the root cause of particular emissions is not well understood. The alkyl-SiNPs synthesised were subjected to testing of surface chemistry and elemental composition through x-ray photoelectron spectroscopy (XPS), and previously reported correlations between

photoluminescence and the presence of nitrogen and oxygen containing species was shown not to be true in the case of these particles.

The one-pot chemical synthesis method for alkyl terminated SiNPs investigated and reported here is simple, cheap and easily scalable. In addition, toxic reagents involved in other contemporary synthesis methods for similar particles are not required. The SiNPs produced are of consistent size and high stability, with a strong photoluminescence emission. The simplicity of the synthesis ensures that the method can be easily employed in the future to introduce other more complex surface groups and this method has the potential to greatly combat the inherent problems in large scale SiNP synthesis.

Contents

List of figures	VIII
List of tables	XI
Abbreviations	XII
1 General Introduction	1
1.1 Introduction.....	1
1.2 Semiconductor nanoparticles.....	2
1.2.1 <i>The Quantum Confinement effect</i>	2
1.2.2 <i>Silicon nanoparticles</i>	4
1.3 SiNPs: synthesis discussion.....	4
1.3.1 <i>Top-down methods: electrochemical etching</i>	5
1.3.2 <i>Bottom-up methods: Solution synthesis and inverse micelles</i>	6
1.4 Functionalisation	6
1.5 Applications of Semiconductor nanoparticles.....	8
1.5.1 <i>Biological applications</i>	8
1.5.2 <i>Applications in thermoelectric materials</i>	9
1.5.3 <i>Photovoltaic applications</i>	10
1.6 Thesis overview	11
2 Methods and materials.....	13
2.1 Synthesis of alkyl-SiNPs	13
2.1.1 <i>Methanol quenched synthesis and work up</i>	14
2.1.2 <i>CuCl₂ quenched synthesis and work up</i>	17
2.2 Characterisation of alkyl-SiNPs.....	20
2.2.1 <i>Optical measurements</i>	20
2.2.2 <i>Size and dispersity measurements</i>	21
2.2.3 <i>Chemical analysis</i>	23
3 Characterisation of alkyl functionalised SiNPs	25
3.1 Introduction.....	25
3.2 Alkyl-SiNP characteristics:	25

3.2.1	<i>FTIR and NMR: particle surface analysis</i>	25
3.2.2	<i>TEM and DLS: particle size and structure</i>	29
3.2.3	<i>PL and UV-Vis: optical properties</i>	35
3.3	Summary.....	40
4	Quenching with CuCl₂: particle characterisation	41
4.1	Introduction.....	41
4.2	Alkyl-SiNP characteristics	41
4.2.1	<i>FTIR and XPS: particle surface analysis</i>	41
4.2.2	<i>TEM, STEM and DLS: particle size and structure</i>	49
4.2.3	<i>PL and UV-Vis: optical properties</i>	57
4.3	Summary.....	60
5	Conclusions and future work	61
6	References and publications	64
6.1	References.....	64
6.2	Publications	69

List of figures

Figure 1: The different possible applicable energy level diagrams for a semiconductor in different phases.	3
Figure 2: Reaction scheme showing the formation of alkyl-SiNPs with undesirable methoxy capping as a side reaction.....	16
Figure 3: Reaction scheme showing the formation of alkyl-SiNPs. Excess reducing agent is removed through the use of CuCl_2 dispersed in the reaction mixture.....	19
Figure 4: a) – c) FTIR spectra for hexyl, octyl and dodecyl capped SiNPs respectively using MeOH quenching method. d) – f) the same samples respectively with measurements taken one week after graphs a) – c).	27
Figure 5: $^1\text{H-NMR}$ spectra for octyl capped SiNPs after being quenched with methanol. Sample was dispersed in CDCl_3 solvent.....	28
Figure 6: TEM images of a) hexyl, b) octyl and c) dodecyl capped SiNPs produced via the methanol quenching reaction. Particles highlighted with red circles in a) and b) for clarity.....	32
Figure 7: Hydrodynamic diameter expressed by number for alkyl-SiNPs a) hexyl, b) octyl and c) dodecyl produced by the MeOH quenched method.	35

Figure 8: UV-Vis spectra for hexyl capped SiNPs produced from the methanol quenching mechanism, showing an indirect bandgap transition at a wavelength of 330 nm.36

Figure 9: PL emission and excitation spectra for a) Hexyl, b) octyl and c) dodecyl capped SiNPs produced via the methanol quenching option. d) shows a real colour image of a solution of dodecyl capped SiNPs suspended in Hexane when subjected to a 325 nm wavelength UV light source.39

Figure 10: a) FTIR spectrum of a SiNP sample produced by this modified method but without any additional purification techniques showing broad salt peak at 3000 to 3500 cm^{-1} . b) FTIR spectrum of the same sample once additional purification techniques have been used. c) FTIR spectrum of the same sample + 1 week showing stability.....44

Figure 11: XPS surface elemental analysis of a sample of dodecyl-SiNPs. a) Survey spectrum of all elements, b) silicon peak (Si2p), c) oxygen peak (O1s), d) carbon peak (C1s), e) no peak, background only in nitrogen (N1) region, f) no peak, background only in copper (Cu2p) region.49

Figure 12: Hydrodynamic diameter expressed by number for alkyl-SiNPs a) hexyl, b) octyl and c) dodecyl produced by the CuCl_2 quenched method.51

Figure 13: TEM images of a) hexyl, b) octyl and c) dodecyl capped SiNPs produced via the CuCl_2 quenching reaction. Some particles are highlighted with red circles for clarity.....54

Figure 14: STEM images of hexyl-SiNPs. a) standard image of sea of particles, b) high resolution close up image of a single particle, demonstrating 0.31 nm crystalline silicon lattice fringe spacing.....57

Figure 15: PL emission and excitation spectra for a) hexyl, b) octyl and c) dodecyl capped SiNPs produced via the CuCl_2 quenching option. d) shows a real colour image of a solution of dodecyl capped SiNPs suspended in Hexane when subjected to a 325 nm wavelength UV light source.....59

List of tables

Table 1: Quantities and concentrations of alkyl capping agents/surfactants used in the synthesis of alkyl-SiNPs.....14

Table 2: Silicon core sizes and standard deviations for each of the three particle types produced by the MeOH quenched method.33

Table 3: Silicon core sizes and standard deviations for each of the three particle types produced by the CuCl₂ quenched method.55

Abbreviations

a.u.	Arbitrary units
ATR	Attenuated total reflectance
BE	Binding energy
CDCl_3	Deuterated chloroform
CPS	Counts per second
CuCl_2	Copper (II) chloride
DLS	Dynamic light scattering
eV	Electron volt
FTIR	Fourier-transformed infra red
g	Grams
in vacuo	In a vacuum
LiAlH_4	Lithium aluminium hydride
M	Molar
mbar	Milli bar
mL	Milli litre
mm	Milli meter
mmol	Milli mole
nm	Nano meter
NMR	Nuclear magnetic resonance
PL	Photoluminescence
ppm	Parts per million
PVDF syringe filter	Polyvinylidene fluoride membrane syringe filter

QD	Quantum Dot
SiCl ₄	Silicon tetrachloride
SiNP	Silicon nanoparticle
STEM	Scanning transmission electron microscope
TEM	Transmission electron microscope
UHV	Ultra-high vacuum
UV	Ultra-Violet
UV-Vis	Ultra-Violet / Visible
XPS	X-ray photoelectron spectroscopy

1 General Introduction

1.1 Introduction

A modern and exciting field of science, nanotechnology deals with the development of novel materials consisting of particles with sizes in the nanometer scale, 1-1000 nm, with nanoparticles in particular being amongst the smallest nanomaterials typically between 1-100 nm in diameter. These nanomaterials are less bound by the classical mechanics of their bulk phase companions and demonstrate exciting quantum effects.¹ Determining the nature of these quantum effects is an exciting scientific challenge, and the resulting nanomaterials have amazing potential applications in a broad variety of fields from and bio-imaging² to thermoelectric power generation.³ Nanomaterials take on many forms throughout the body of research. For example, they may be thin films, particles or wires; they may be inorganic metals or organic materials. The focus here is on semiconductor nanoparticles.

1.2 Semiconductor nanoparticles

Semiconductor nanoparticles, or quantum dots (QDs) are of particular interest in research. These particles typically have the smallest diameters of nanoparticles, being only 1-20 nm in size, and as a consequence of this demonstrate unique physical properties.⁴ Small semiconductor nanoparticles demonstrate quantum confinement effects which are amplified with particles of diminishing size through an increase of the band gap. In addition, smaller particles have an increased surface to volume ratio which exemplifies the particles surface properties.⁵ Therefore, the ability to control physical, electronic and chemical properties when synthesising these particles is paramount. This control is achieved through the use of appropriate synthetic methods.

1.2.1 The Quantum Confinement effect

In the case of the smallest nanoparticles – typically less than 10 nm in diameter, the quantum confinement effect refers to a semiconductor material whose diameter is smaller than the size of its exciton Bohr radius.⁶ The effect results in optical and electronic properties that are largely different from those of the bulk phase, and such properties have been shown to occur in a number of semiconductor nanoparticles.⁷⁻¹⁰

The quantum confinement effect is often described in terms of the “particle in a box” model,¹¹ and aids in the understanding of the band gap transitions of semiconductor nanoparticles. The continuous band of a bulk material separates into

discrete energy levels, with the energy gap widening as the size of the particle decreases (Figure 1).¹² With a trapped electron there is increased certainty of position, and where in the bulk phase transitions can occur at a myriad of close energy states, the confined energy levels of a semiconductor nanoparticle result in singular precise transitions,¹² which results in the interesting optical properties and PL observed in such materials.

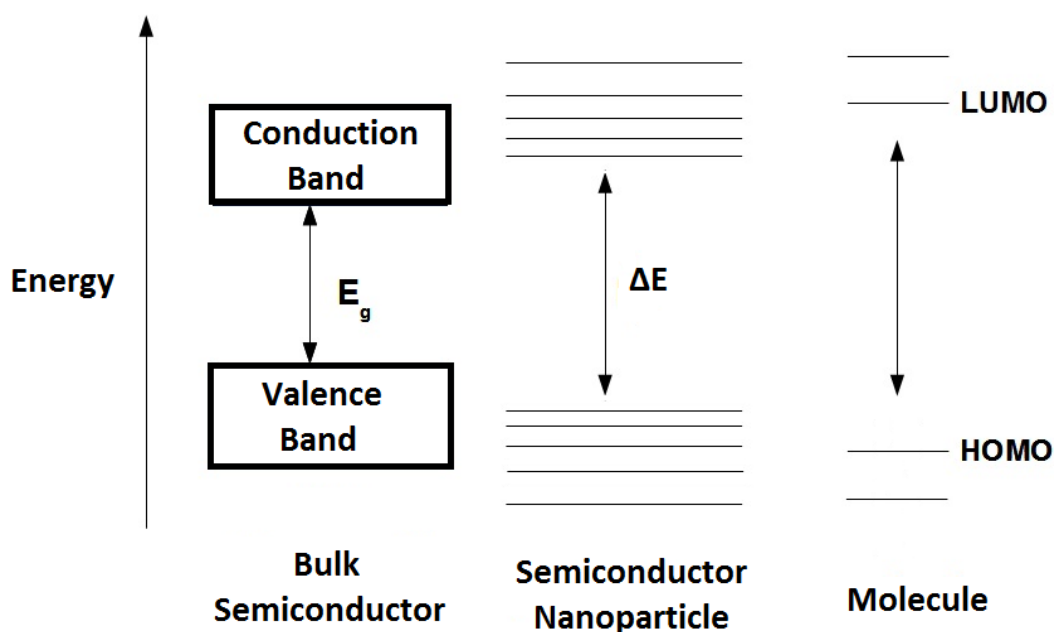


Figure 1: The different possible applicable energy level diagrams for a semiconductor in different phases.

The PL properties of quantum dots provides these materials with the benefits of things such as organic dyes, opening up a number of possible roads of application.

1.2.2 Silicon nanoparticles

The most commonly utilised nanoparticles are based in groups II – VI of the periodic table, which often exhibit an inherent toxicity, such as cadmium selenide particles.¹³ In comparison, silicon is not inherently toxic in this fashion, and is naturally very stable. Silicon has a great many bulk applications but has found limited use in the nanoscale due to its restrictive optical properties. The electronic transition from the valence to the conduction band is possible only as an indirect transition.¹⁴ this transition rarely occurs, and is due to the small size and surface termination of the particles as part of the quantum confinement effect described above.¹⁵

1.3 SiNPs: synthesis discussion

The primary goal of SiNP synthesis is to obtain particles with physical and chemical properties suitable for their required purpose. Many methods for SiNP synthesis have been proposed since the first method was devised in 1992 by Heath et al.¹⁶ with the main goal being to synthesise particles with a desirable size and surface termination. These results should also be achieved by the most efficient means possible. The synthesis method should be safe, cheap and easily scalable. Every method that is proposed has its own unique strengths and weaknesses in these different areas. Generally speaking synthesis methods are categorised as either “Top-down” or “Bottom-up”. I.e. either bulk silicon is broken down into nanoparticles or they are constructed atom by atom respectively.

1.3.1 Top-down methods: electrochemical etching

One of the clearest routes to SiNP synthesis is to break down bulk silicon. This can be achieved through a process of electrochemical etching of a silicon wafer. This produces porous silicon which exhibits quantum confinement properties and PL efficiency as first demonstrated by Leigh Canham in 1990.¹⁷ Sonication of the porous silicon can break it up into nanoparticles, but precise size control by this method was initially difficult to achieve, as demonstrated by Heinrich et al.¹⁸ Particles produced using this method primarily show a bright red or orange luminescence, but since then control over the size of the particles has allowed for tuneable optical properties.¹⁹ The earliest examples of SiNPs produced by this method were hydrogen terminated or “bare”. In 2002, Lie et al.²⁰ were able to cap particles produced from porous silicon with a hydrocarbon surface layer, thus protecting the otherwise unstable surface chemistry and allowing the particles to be easily dispersed in organic solvent.²¹

Top-down electrochemical etching is an example of a route which has been pursued extensively in SiNP research. However, it is not an ideal approach. Etching involves the use of a highly toxic fluoride media, and the system is not easily scalable. In this regard, bottom-up synthesis offers more opportunity to tailor the synthetic approach.

1.3.2 Bottom-up methods: Solution synthesis and inverse micelles

Solution synthesis is a chemical bottom-up approach. The field was pioneered by Kauzlarich et al.²² from 1996 when the first proposed solution synthesis was published. This method however was not without its problems, lacking in size control and yield just like the top-down counterpart. Wilcoxon et al.²³ produced very small crystalline SiNPs with size monodispersity in 1999, and accomplished this by forming inverse micelles, a technique that inspired future solution synthetic methods in this field. Tilley et al.²⁴ was the next step in inspiration for this work, producing SiNPs by reducing silicon tetrachloride (SiCl₄) with hydride. In 2011 Wang et al.²⁵ released a communication that was the direct initial inspiration for the work presented below. Here, SiNPs had their surface terminations controlled directly from the reactants, forming inverse micelles and producing an alkyl passivated surface chemistry. However, their product showed poor stability apparently due to oxidation.

1.4 Functionalisation

As mentioned above. SiNPs may be described as “bare” when they are produced without surface modifications of any kind. In this case the particles surface is hydrogen terminated, and this leaves the particles in a highly reactive state. This primarily leads to particle agglomeration and leaves the surfaces open to oxidative attack.

Stabilization of the SiNPs involves surface functionalisation and thus protection through the formation of covalent bonds. A natural method of accomplishing this is a hydrosilylation reaction, whereby an unsaturated hydrocarbon reacts with the SiNPs hydrogen terminated surface whilst leaving the Si-Si bonds of the particle core unaffected.²⁶ The protection of the particles with surface functionalisation has also been shown to preserve PL intensity and prevent particle oxidation in air, thus improving overall SiNP stability and lifetime, as shown by Li et al.²⁷

A number of different approaches to particle functionalisation have been tested and proven, with invaluable consequence. Particle capping with polar or non-polar groups makes them soluble in polar or non-polar solvents respectively,^{20, 28} and particular particle functionality influences the possible particle applications.

In this regard, particles that are formed bare and then subject to a later functionalisation step are open to the possibility of contamination by unwanted species, a most common problem being oxidisation in air. The work started by Wang et al.²⁵ and expanded below aims to form the SiNPs in a one pot synthesis which introduces surface capping as the particles are formed due to the employment of an inverse micelle structure.

1.5 Applications of Semiconductor nanoparticles

The potential applications of SiNPs are determined by the above discussed unique and novel properties. The size and surface functionality of the particles has been shown to give rise to optical and electrical properties that make SiNPs possible options for a number of fields of application, and this coupled with the abundance and low toxicity of the core material makes them an approachable option.

1.5.1 Biological applications

In biology, the small size of nanoparticles makes them very compatible with biological systems. This natural potential has led to a great deal of research in the field, particularly in the fields of cancer therapy and diagnosis.^{29, 30} A limiting factor however, is the inherent cytotoxicity of many of the available nanoparticles; this behaviour has been extensively studied.^{31, 32} In particular however, Shiohara et al.⁸⁸ have shown that SiNPs are an excellent candidate for low toxicity QD's. Their surface functionality can be tailored to be hydrophilic and their PL emission is in the visible range, which is ideal for imaging.² In particular, Warner et al.³³ have shown a resistance of SiNP PL to photobleaching greater than that of the currently employed organic dyes. An area of research currently being investigated for SiNPs is a step on from the diagnostic imaging usage in order to also incorporate direct targeting and drug delivery systems for direct cancer thereapy.³⁴

1.5.2 Applications in thermoelectric materials

Currently of great interest in the fields of physical chemistry and materials science, thermoelectric materials are solid state heat engines which convert temperature gradients into electrical energy and vice versa; without mechanical intervention. This is by virtue of the characteristic flow of 'free' electrons of the semiconductor metals inside such devices. There are a great many possible applications for thermoelectric devices, with a broad variety in scale and market. Applications have been suggested for military equipment, aviation and medical treatment as well as taking advantage of the Peltier effect in small scale consumer refrigeration products, such as mini/car coolers hotel fridges etc. Other, more industrial 'waste heat' processes include energy scavenging from outdoor boilers, industrial furnaces, oil and gas fields etc.³⁵

With extremely small particles, strong electrical conductivity can be maintained whilst thermal conductivity is limited, due to the introduction of grain boundaries causing high phonon scattering. This combination of conditions is required to gain the highest thermoelectric efficiencies. Cutting edge thermoelectric research is investigating new materials which tailor these properties individually; with some excellent laboratory results – including vast improvements decreasing the thermal conductivity in Silicon nanowires and thin films.^{3,36} Recently, Work by Ashby et al.³⁷ in 2012 produced phenylacetylene-capped SiNPs doped with charge carriers in order to produce measurable thermoelectric properties.

The conversion of heat energy into electricity is also an interesting possible addition to the use of silicon in similar photovoltaic applications.

1.5.3 Photovoltaic applications

Silicon is already used extensively in the field of photovoltaics, whereby electrical power is generated from light. With the growing popularity of this technology research into improving its efficiency is of paramount importance. The incorporation of silicon nanoparticles into solar cells and the application of thin films is a recent development with proven results.³⁸

1.6 Thesis overview

The purpose of this thesis is to develop and optimise a simple, cheap, efficient and easily scalable one-pot synthesis of alkyl-functionalised silicon nanoparticles using a bottom-up inverse micelle based method. In addition, the thesis gives an overview of the size and surface chemistry of the particles, as well as an insight into the nature of their observed optical properties.

Chapter 1 begins with a general introduction to the field of nanotechnology, semiconductors, and in particular silicon nanoparticles. It details the two possible routes that can be taken to synthesize such particles, bottom-up and top-down, and gives examples of possible synthesis routes for each of these paths that are regularly employed in current research, as well as highlighting some limitations. The origin of SiNPs unique PL properties is also discussed, as well as the importance of particle surface chemistry and size. Finally, the broad implications of research in this field are highlighted with a discussion of a number of exciting possible applications.

Chapter 2 details the materials and methods used in each stage of the experimental and analytical work. The syntheses analysed in chapters 3 and 4 are detailed as well as the specifications and procedures for instruments used in characterisation.

In Chapter 3, methods first demonstrated by Wang et al.²⁵ are explored and improved upon, and a new method for the synthesis of alkyl-SiNPs via a simple one-pot synthesis is presented. The particles produced are characterised via a number of spectroscopic techniques and the surface chemistry and optical properties are discussed. Particle stability is shown to be high, and surface oxide interpreted by

previous studies as particle instability and oxygenation in air is reattributed to alkoxy capping as a by-product of quenching the reaction with alcohol.

Chapter 4 leads on from the discoveries of chapter 2 and aims for an alternative approach to quenching the reaction in order to eliminate the undesirable alkoxy surface functionality. This approach involves the use of CuCl_2 , to quench the reducing agent but leads to its own complications in terms of yield and purity of product. Here the resulting particles are also examined with respect to their size, surface chemistry and optical properties.

Chapter 5 concludes and summarizes the thesis, outlining the achievements and limitations of the proposed synthesis methods and possible other courses of action on the topic and future work. In particular, at this point the nature of the observed optical properties of the produced SiNPs is discussed and compared with a recent publication by Dasog et al.³⁹

References used in the thesis and publications to which I have contributed are listed in chapter 6.

2 Methods and materials

Presented below is a detailed description of the practical methods, chemicals and procedures used for the bottom-up solution synthesis of alkyl-SiNPs. The methods of characterisation and equipment used to determine the physical and optical properties of the product are also described in detail.

Materials: toluene (Fisher, 99.9 %) dried over sodium wire; methanol (Sigma-Aldrich, 99.8 %); hexane (Fisher, 99.9 %); lithium aluminium hydride solution (Fisher, 1 M in THF); silicontetrachloride (Sigma-Aldrich, 99 %); trichloro(hexyl)silane (Sigma-Aldrich, 97 %) stored under N₂; trichloro(octyl)silane (Sigma-Aldrich, 97 %) stored under N₂; trichloro(dodecyl)silane (Sigma-Aldrich, 95 %) stored under N₂; anhydrous copper (II) chloride (Sigma-Aldrich, 99%).

2.1 Synthesis of alkyl-SiNPs

The following methods are the final optimised approach. Previous work in the subject and the foundation of this method is based on the work reported in “The effect of alkyl chain length on the level of capping of silicon nanoparticles produced by a one-pot synthesis route based on the chemical reduction of micelle” *listed under Chapter 6.2: Publications.*

To ensure that the results could be consistently replicated with varying surface functionality 3 types of alkyl-SiNP were produced using hexyl, octyl and dodecyl surface moieties.

2.1.1 Methanol quenched synthesis and work up

Toluene (50 ml) is degassed by 5 minutes pulsed sonication under vacuum. 0.5 mL SiCl_4 is then introduced, followed by an alkyl- SiCl_3 surfactant in the quantities given in Table 1.

Table 1: Quantities and concentrations of alkyl capping agents/surfactants used in the synthesis of alkyl-SiNPs

Surfactant Name	Quantity /mL	Concentration (/mmol)
Hexyltrichlorosilane	0.80	4.03
Octyltrichlorosilane	0.93	4.02
Dodecyltrichlorosilane	1.20	4.03

The solution is then dispersed by one minute of vigorous shaking followed by continuous sonication for 60 minutes, during this time a SiCl_4 core is formed and surrounded by the alkyl surfactant to form a hydrophobic inverse micelle system, with the alkyl chain as the distal moiety. A reducing agent, 4 mL LiAlH_4 – 1 molar solution in THF, is then added dropwise, giving vigorous hydrogen bubbling and the formation of an insoluble white precipitate. This solution is then sonicated for 120 minutes in order to reduce Si-Cl bonds to Si-Si. 20 mL methanol is then slowly added to the reaction mixture to quench any excess LiAlH_4 , again accompanied by the expulsion of hydrogen gas. The reaction is brought to completion by 60 minutes of sonication. Solvent is then removed in vacuo, resulting in a white powder (by-products) and clear gel/oil (desired nanoparticles) system. The product is re-

dispersed in 20 mL hexane with 5 minutes sonication, and any remaining by-product is filtered out using a PVDF syringe filter (450 nm). The solution can then be dried in vacuo to leave a clear, pale yellow gel/oil product. Typical yield is approximately 0.7 g.

This process is illustrated in Figure 2 below, which also shows other possible moiety's occurring as a consequence of incomplete capping. This includes the reduction of any surface Si-Cl bonds to Si-H bonds, and possible surface oxidation of these Si-H bonds to form methoxy groups.

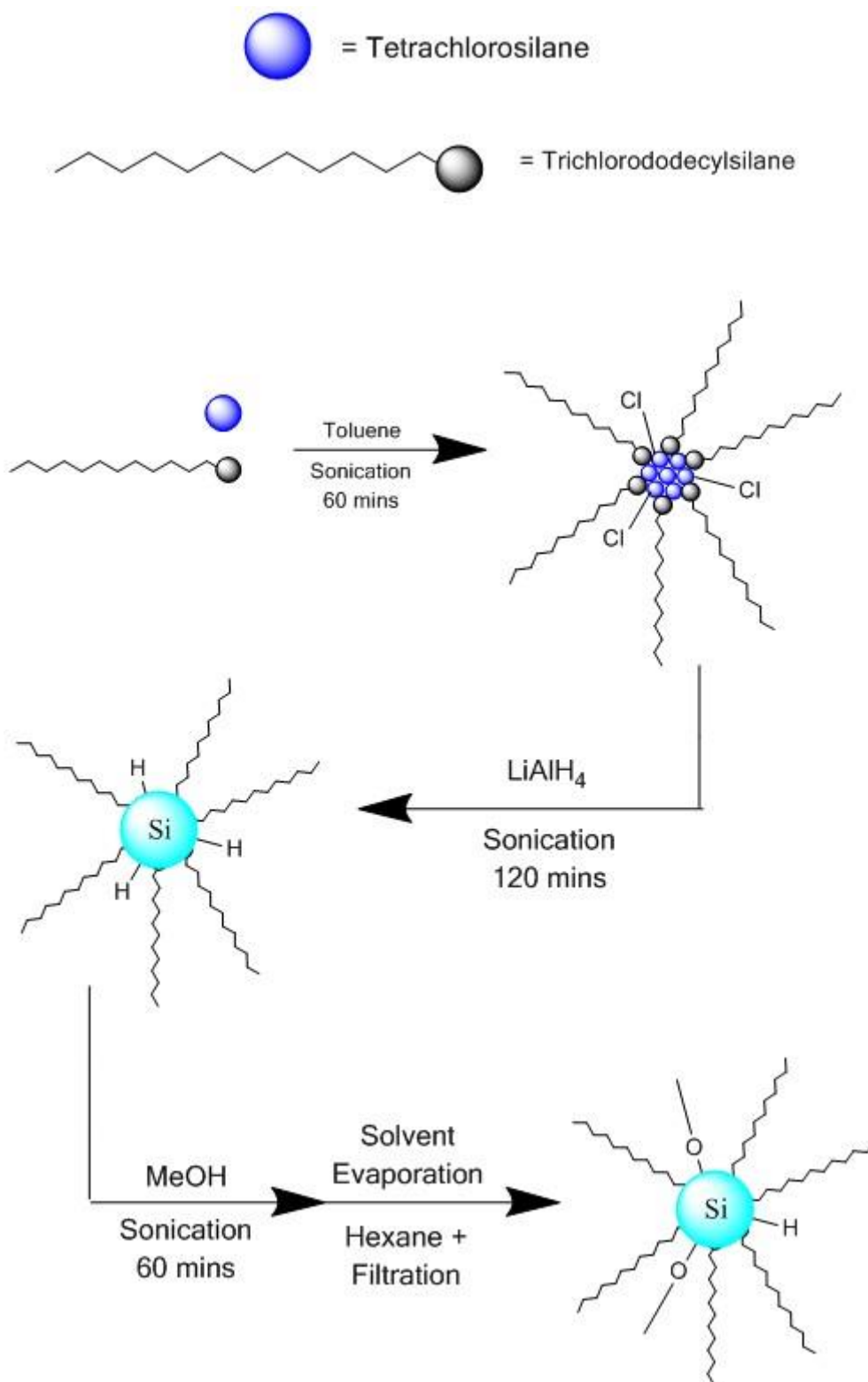


Figure 2: Reaction scheme showing the formation of alkyl-SiNPs with undesirable methoxy capping as a side reaction.

The results of this optimisation of our previous work are shown in detail below, but in summary, although undesirable Si-H surface functionalisation appears dramatically reduced, if not eliminated surface oxidation due to alcohol use remains a problem. This issue is addressed in the following method, whereby the use of anhydrous copper (II) chloride replaces that of methanol when quenching excess LiAlH_4 .

2.1.2 CuCl_2 quenched synthesis and work up

In this case, for the most part the method is the same as the one detailed above. toluene (50 ml) is degassed by 5 minutes pulsed sonication under vacuum. 0.5 mL SiCl_4 is then introduced, followed by an alkyl- SiCl_3 surfactant in the quantities given in Table 1. The solution is then dispersed by one minute of vigorous shaking followed by continuous sonication for 60 minutes, during this time a SiCl_4 core is formed and surrounded by the alkyl surfactant to form a hydrophobic inverse micelle system, with the alkyl chain as the distal moiety. A reducing agent, 4 mL LiAlH_4 – 1 M solution in THF, is then added dropwise, giving vigorous hydrogen bubbling and the formation of an insoluble white precipitate. This solution is then sonicated for 120 minutes in order to reduce Si-Cl bonds to Si-Si.

Instead of continuing as reported above, at this point 1.5 g anhydrous CuCl_2 powder is added to the reaction mixture. The copper chloride again quenches any excess LiAlH_4 – accompanied by the expulsion of hydrogen gas – but does not cause any undesirable particle surface functionality. This mixture is shaken vigorously and then

sonicated for 60 minutes. The product produced is a gel/oil similar to that which is described above. However, this is now mixed with remaining unreacted CuCl_2 , and salt by-products. Therefore, numerous purification steps are required; the mixture is filtered twice under reduced pressure in order to remove large amounts of solid by-products. The result is a pale yellow/orange solution, including remaining by-product, particles and solvent. The solvent is then removed in vacuo, resulting in a yellow/white solid by-product and clear gel/oil product system. This product is then re-dispersed in 6 mL petroleum ether via 5 minutes sonication and is separated by 60 minutes centrifugation at 7000 rpm. The upper liquid layer is then decanted, filtered using a PVDF syringe filter (450 nm) and dried in vacuo. The resulting product is a pale yellow gel/oil as above, with a typical yield of 0.3 g. This yield is lower than that of the previous method due to an increased loss of product in the more complex purification procedures. The above synthesis method is shown in Figure 3 below.

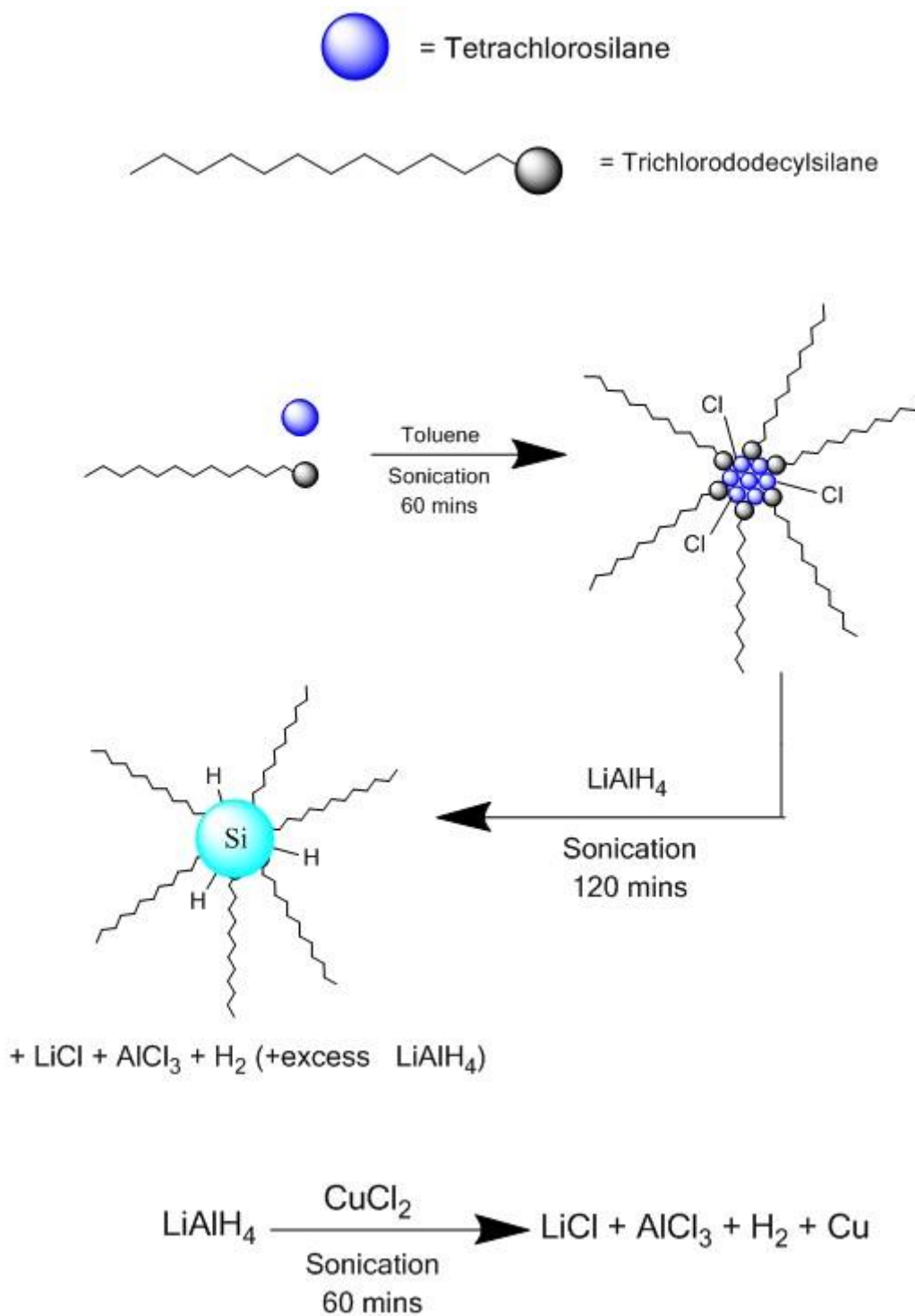


Figure 3: Reaction scheme showing the formation of alkyl-SiNPs. Excess reducing agent is removed through the use of CuCl_2 dispersed in the reaction mixture.

2.2 Characterisation of alkyl-SiNPs

The following is an account of the methods used to gather detailed physical and optical data on alkyl-SiNPs synthesised as above. The characteristics discovered are very different from the materials properties in the bulk phase, and techniques are not always well optimised for dealing with products on the nanoscale. In this regard, a broad range of techniques has been employed to build an image of the properties of particles produced.

2.2.1 *Optical measurements*

The following measurements were performed on all samples in normal room temperature and pressure conditions.

2.2.1.1 Fluorescence spectroscopy

Indirect optical transitions in the particles were measured with photoluminescence spectra, which were taken for samples dissolved in hexane in a quartz cuvette (10 mm x 10 mm), using a Perkin-Elmer LS55 spectrophotometer with emission slit width of 5 nm; wavelengths below 390 nm are cut out in the emission spectrum for clarity. In each case, the excitation wavelength used in the emission spectrum corresponds to the excitation spectrum maximum, and vice versa, iterating to get the optimum result. Initial photoluminescence spectra were taken with an excitation wavelength as indicated by UV-Vis spectra.

2.2.1.2 Ultraviolet-visible spectroscopy

Ultra-violet/visible absorption spectra were obtained for samples dissolved in hexane in a quartz cuvette (10 mm x 10 mm). The spectrometer used was a Perkin-Elmer 35 UV-Vis double-beam spectrophotometer. The scan range was 200 - 700 nm at a rate of 480 nm min⁻¹. The background was corrected by division of a spectrum of blank hexane solvent, as per the Beer-Lambert law.

2.2.2 *Size and dispersity measurements*

In the first instance these techniques simply confirm the existence of the particles, either by direct imaging or size measurement. However, further information regarding particle morphology is valuable when considering longer term applications of the product.

2.2.2.1 Transmission electron microscopy

Transmission electron microscopy (TEM) is a technique whereby a focussed beam of electrons is transmitted through a thin sample. Due to their interactions as they pass through the matter images determined by contrast are given. Where electrons are unable to pass through the sample darker regions are imaged. Samples were visualised on a JOEL 2000EX with accelerating voltage of 200 kV. A suspension of alkyl-SiNPs in hexane was dispersed by sonication and applied to a carbon-coated 300-mesh copper grid and dried in air. For each sample a minimum of 100 particles

across 5 distinct regions was identified and particles imaged and sized. ImageJ software was utilised for image analysis.

For high quality particle imaging STEM images were also taken in order to capture vivid images of individual particles. These images were taken with a Nion UltraSTEM 100 with accelerating voltage of 100 kV using a cold field emission electron source, at University and a corrector capable of neutralizing aberrations up to fifth order. TEM samples were prepared by dropcast SiNPs solution onto graphene substrate. The solvent was evaporated and TEM micrographs were typically taken at different spots of each grid. Samples were baked at 135 °C for approximately 7 hours in a turbo backed vacuum oven prior to STEM imaging to reduce contamination.

2.2.2.2 Dynamic light scattering measurement

Dynamic light scattering (DLS) utilises the properties of Brownian motion in nanoparticles in order to measure their size. Sizing down to 1 nm is possible though accurate results below 100 nm diameters are difficult to confirm, hence why it is important to utilise a number of analysis techniques. In addition, DLS measurements determine how the particle diffuses, and thus measure what is referred to as the hydrodynamic diameter of the particles. This diameter is larger than the actual particle core size which is measured in TEM, so some discrepancy in the results is to be expected. Measurement of the alkyl-SiNPs were performed in pure hexane solvent and particles were prepared by filtration in order to eliminate as many impurities as possible, as well as a few minutes of sonication in order to ensure a good dispersion in the solvent. Scans were performed with a Zetasizer Nano ZS,

whereby the scattered photons, detected under an angle of 173° , gave the relative number distribution of particles.

2.2.3 Chemical analysis

Surface chemistry analysis of the produced particles is of high importance. It determines the success of the proposed synthesis method in terms of particle functionality and stability, and detects unwanted impurities that would have an impact on any potential applications that the particles might have. As previously discussed, particle surface chemistry as well as size has been shown to have an effect on the observed physical properties of the particles, and thus ensuring control over this factor is imperative.

Because nanoparticles do not behave like normal molecules, a number of spectroscopic techniques have been employed in determining surface functionality and particle elemental analysis in order to get the best possible picture of the particles functionalisation.

2.2.3.1 Fourier transform infrared spectroscopy

Fourier transformed – infra red spectra (FTIR) were collected using a Perkin-Elmer Spectrum 100 ATR FTIR spectrometer. The pure gel product was placed on the crystal and measured versus a background spectrum of the clean crystal. This powerful tool identifies a molecules chemical bonds by measuring infrared absorption.

2.2.3.2 ^1H -NMR spectroscopy

Proton nuclear magnetic resonance measurements of samples dissolved in CDCl_3 were taken using a Bruker 500 MHz NMR spectrometer. These samples were measured relative to the aforementioned lock solvent. Samples were scanned 16 times.

2.2.3.3 X-ray photoelectron spectroscopy

X-ray photoelectron spectroscopy is a powerful surface elemental analysis technique whereby a sample is bombarded with X-rays in order to cause electron ejection from the core of surface atoms. For each element these electrons demonstrate a characteristic binding energy with thus provides a characteristic peak in the resultant photoelectron spectrum.

XPS measurements were taken using a -Alpha XPS instrument (Thermo Scientific, East Grinstead, UK). A monochromatic Al K α x-ray source (1486.6 eV) was used with a spot size of 400 μm diameter. A pass energy of 200 eV and step size of 0.4 eV was used for survey spectra, and a pass energy of 40 eV and step size of 0.1 eV was used for high resolution spectra. A few drops of dry SiNP gel were cast onto a clean gold substrate, This was transferred into a load-lock attached to an ultra-high vacuum (UHV) chamber. For all photoemission spectra, the binding energies (BEs) are referred to the Au $4f$ line, as measured on a gold foil in direct electrical contact with the sample, which lies at BE of 87.4 eV. The resultant data was processed with CasaXPS software.

3 Characterisation of alkyl functionalised SiNPs

3.1 Introduction

In this initial stage: 'hexyl', 'octyl' and 'dodecyl' capped SiNPs were produced via an optimised solution synthesis. In the following analysis of the produced particles physical, chemical and optical properties for each of these three synthesised surface chemistries is explored using the analytical techniques detailed in chapter 2.

3.2 Alkyl-SiNP characteristics:

3.2.1 FTIR and NMR: particle surface analysis

The FTIR spectra strongly indicate the formation and desired functionality of SiNPs. Figure 4 a), b) and c) are spectra of particles with hexyl, octyl and dodecyl surface capping respectively. In each case, peaks at 1460 cm^{-1} show the presence of Si-C bonds; C-H bonds in the capping layer are represented by peaks at approximately 2925 cm^{-1} and 2852 cm^{-1} . Notably, peaks at approximately 2148 cm^{-1} are typical of Si-H bonds. These peaks are comparatively very tiny, so as to be almost negligible when compared with the other peaks shown; this indicates excellent surface coverage thanks to the steps taken to optimise this synthesis. In this case, surface oxidation is indicated by the presence of strong peaks at 1084 cm^{-1} and 1190 cm^{-1} which rather dwarf the other peaks, suggesting quite a large amount of Si-O bonds relative to other forms of surface coverage. Of importance is the fact that the position of these peaks indicates Si-O-C bonding from the introduction of methanol

in the quenching step of the reaction which also promotes methoxy capping of the particles as a side reaction.

FTIR spectra of these same samples left for a period of 1 week are indicated by Figure 4 d), e) and f), which again indicate hexyl, octyl and dodecyl surface functionality respectively. These samples show negligible change in FTIR peak intensities. This indicates high particle stability and resistance to any form of degradation or further oxidation due to exposure to atmosphere, contrary to suggestions made by Wang et al.²⁵ above.

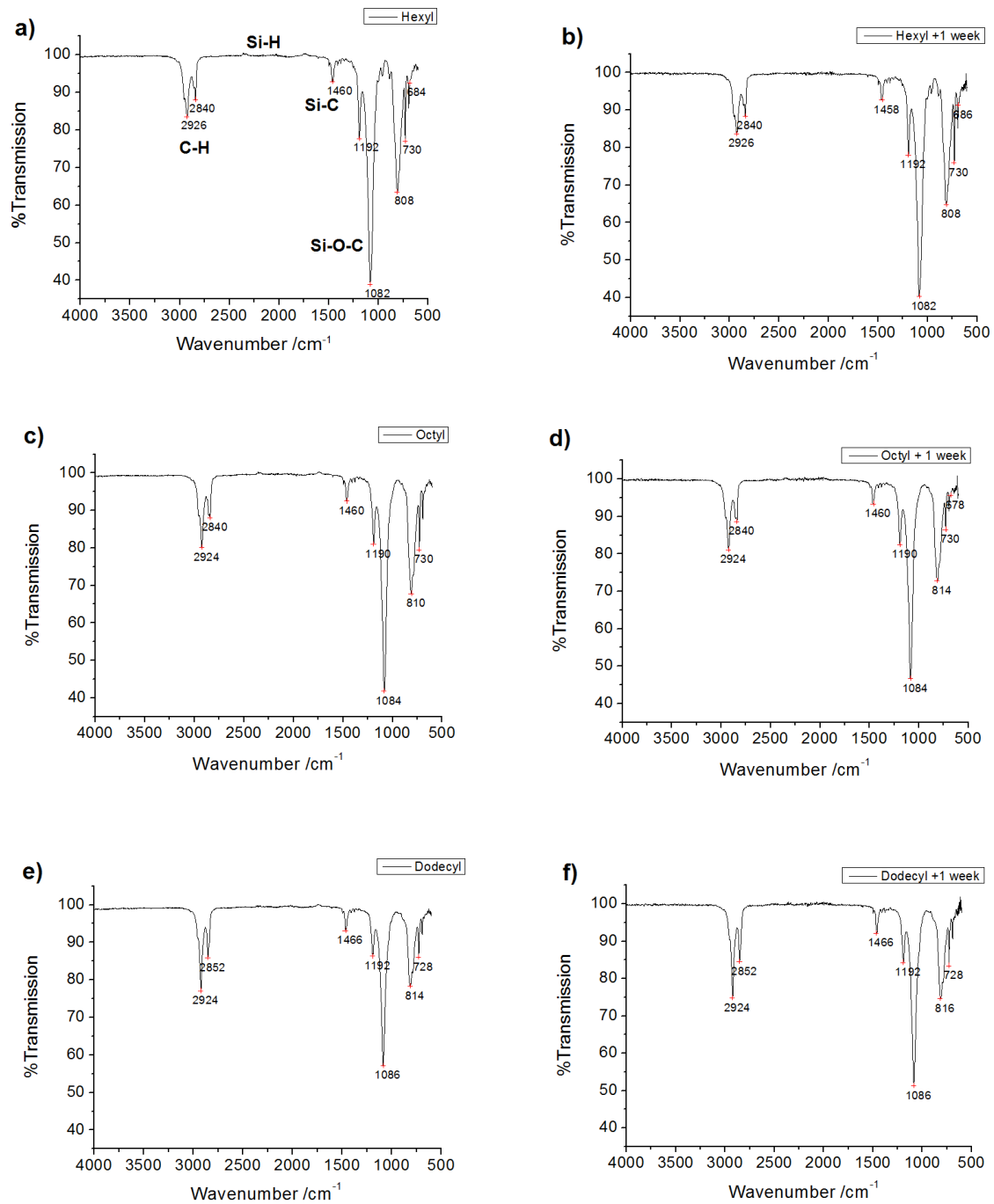


Figure 4: a) – c) FTIR spectra for hexyl, octyl and dodecyl capped SiNPs respectively using MeOH quenching method. d) – f) the same samples respectively with measurements taken one week after graphs a) – c).

When considering proton NMR there are some limitations to the use of the technique on colloidal systems such as this. The particles do not necessarily behave in the way a molecule would. However, despite this potential limitation valuable data has still been gathered for the identification of present surface groups.

Figure 5 below shows proton NMR spectra for the octyl passivated SiNPs.

For the octyl-SiNPs shown in Figure 5 the broadened multiplet observable at ~ 1.3 ppm represents the CH_3 protons as a consequence of the methoxy capping. Also, the alkyl capping is indicated by further peaks, one at ~ 0.5 ppm, characteristic of Si-CH_2 protons, and further CH_2 protons at ~ 1.2 ppm. The final set of CH_3 protons at the end of the alkyl chain are indicated by a peak at ~ 0.8 ppm. A solvent peak at 7.26 ppm has been omitted.

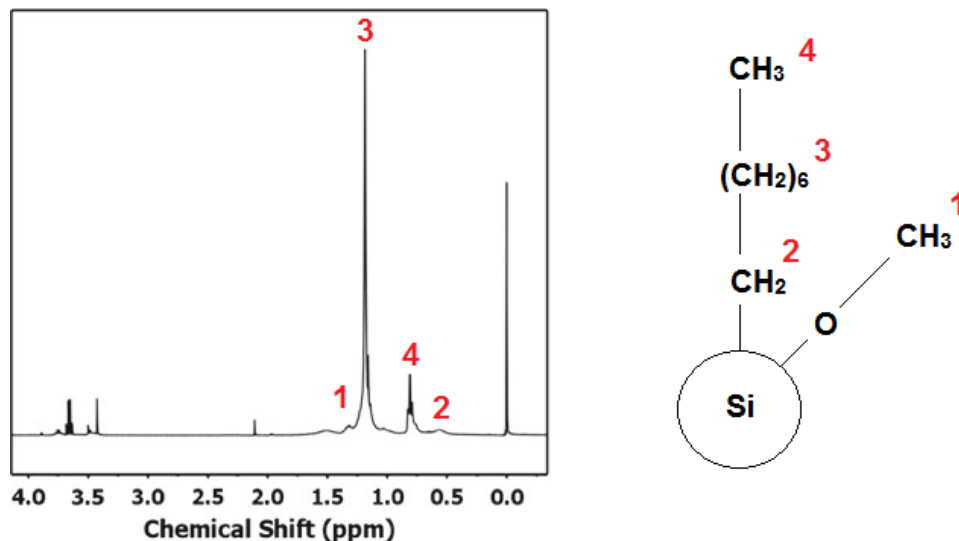
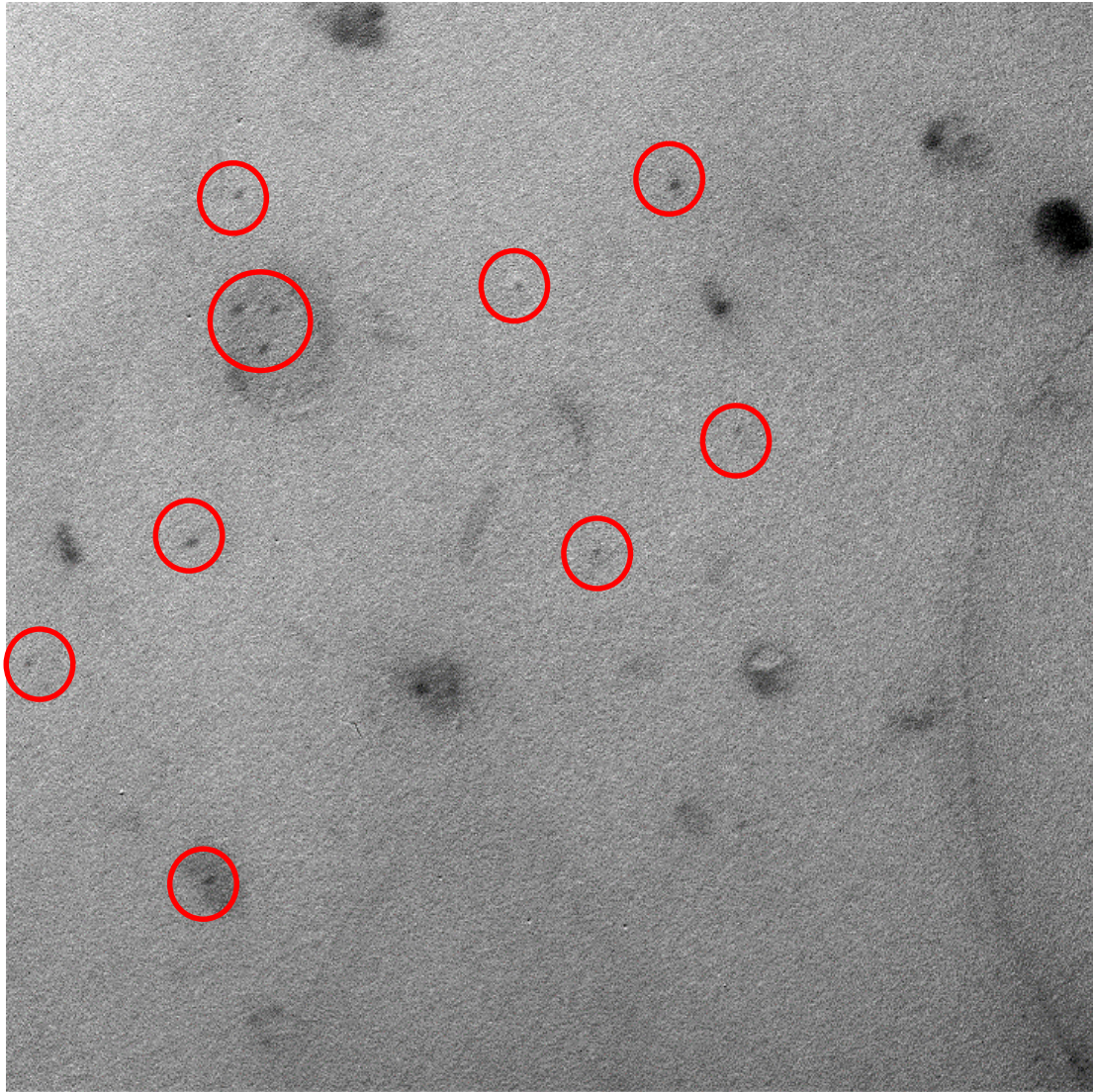


Figure 5: $^1\text{H-NMR}$ spectra for octyl capped SiNPs after being quenched with methanol. Sample was dispersed in CDCl_3 solvent.

3.2.2 TEM and DLS: particle size and structure

Typical TEM images of the 3 produced types of alkyl-SiNPs is shown in Figure 6 a), b) and c). The particles shown, amongst many others, were imaged in this fashion and measured. The particles are well separated and appear to be resistant to agglomeration. Data for the average size and distribution of particles for each of the three ligand types produced is shown in Table 2. It is important to note that these images only show the silicon core due, with the hydrocarbon surface functionality not showing up on the carbon film, and due to low contrast are notoriously difficult to image without the latest in electron microscope technology. Some particles images with a z-contrast STEM system were taken for samples shown in chapter 4.

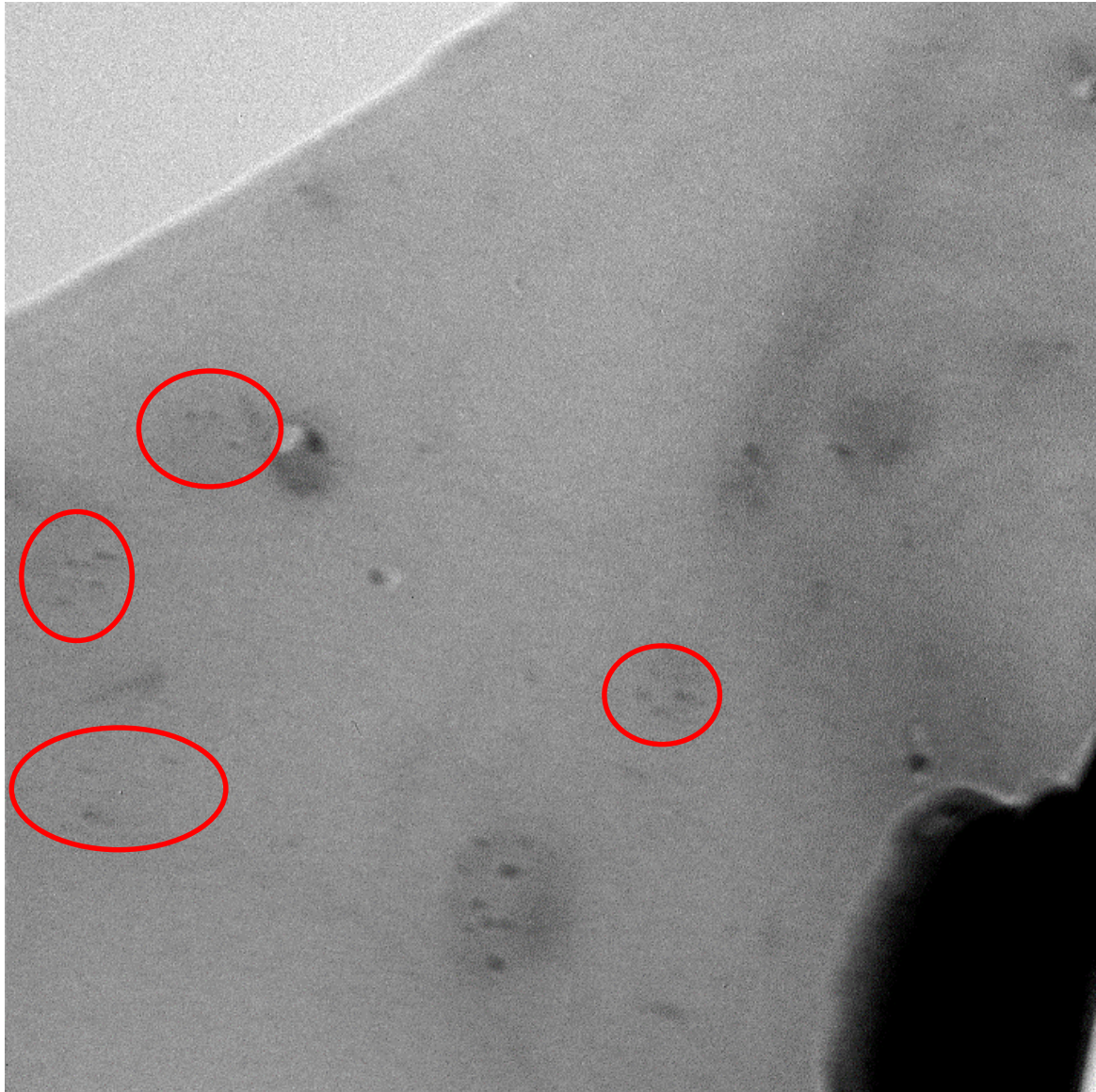
a)



N11.9.tif
TEM Mode: Imaging

100 nm
HV=200.0kV
Direct Mag: 40000x
U.E.A Materials Science

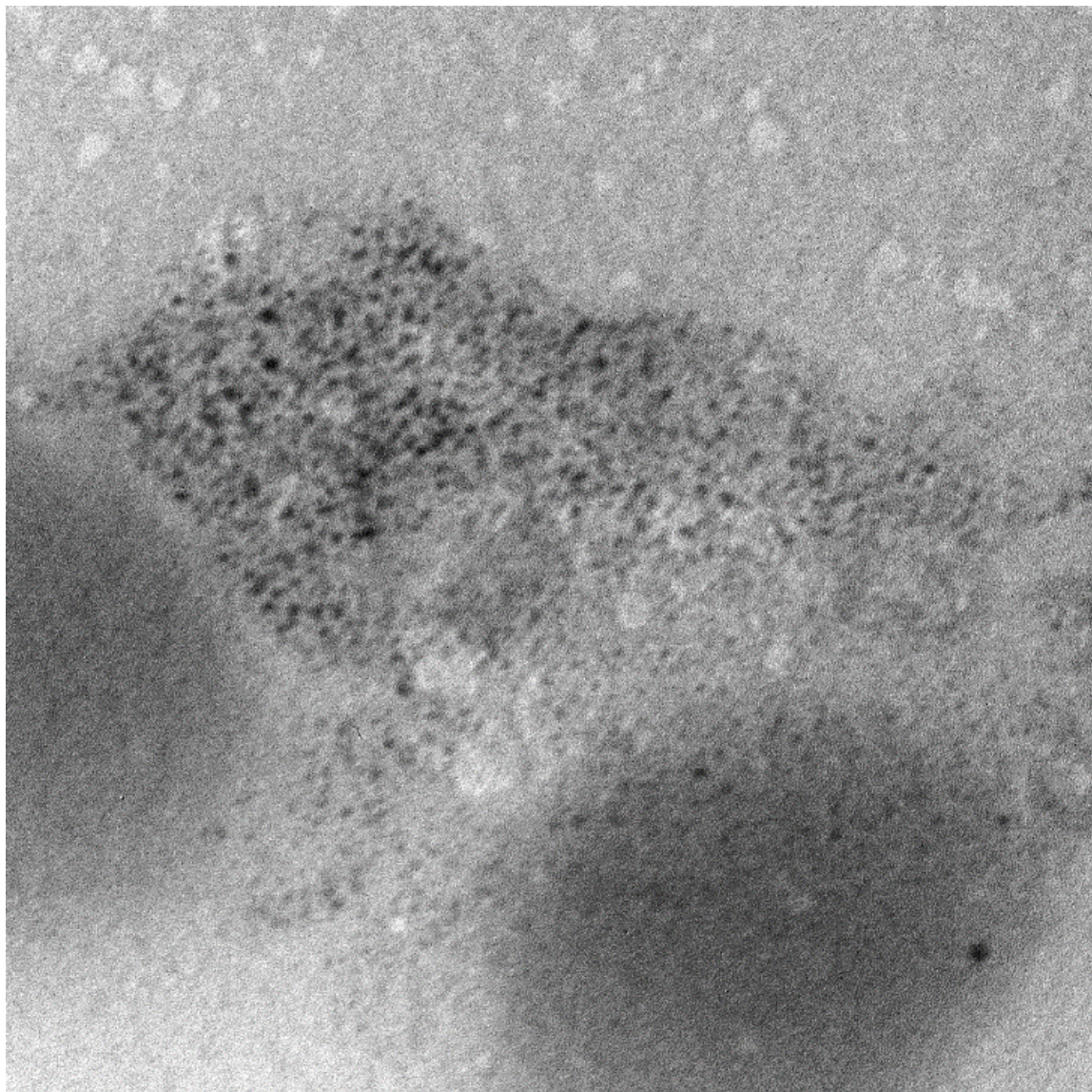
b)



N11.3.tif
TEM Mode: Imaging

100 nm
HV-200.0kV
Direct Mag: 40000x
U.E.A Materials Science

c)



N7.2.tif
TEM Mode: Imaging

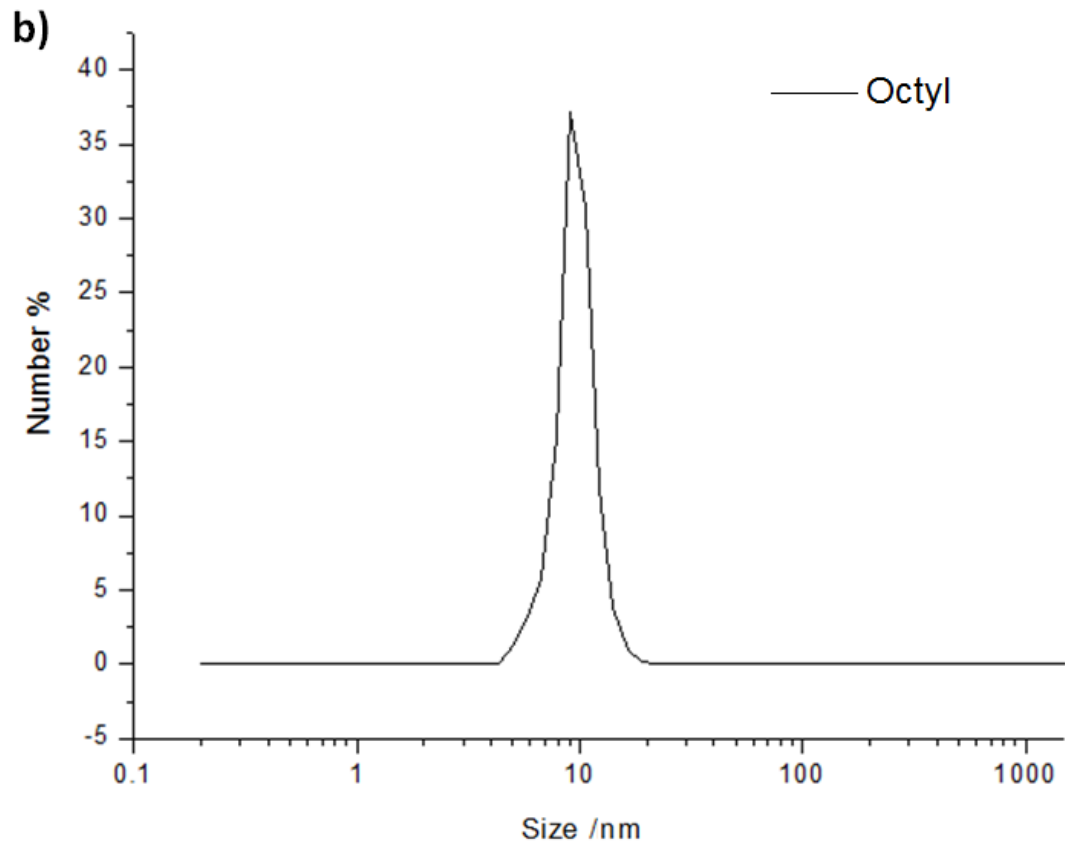
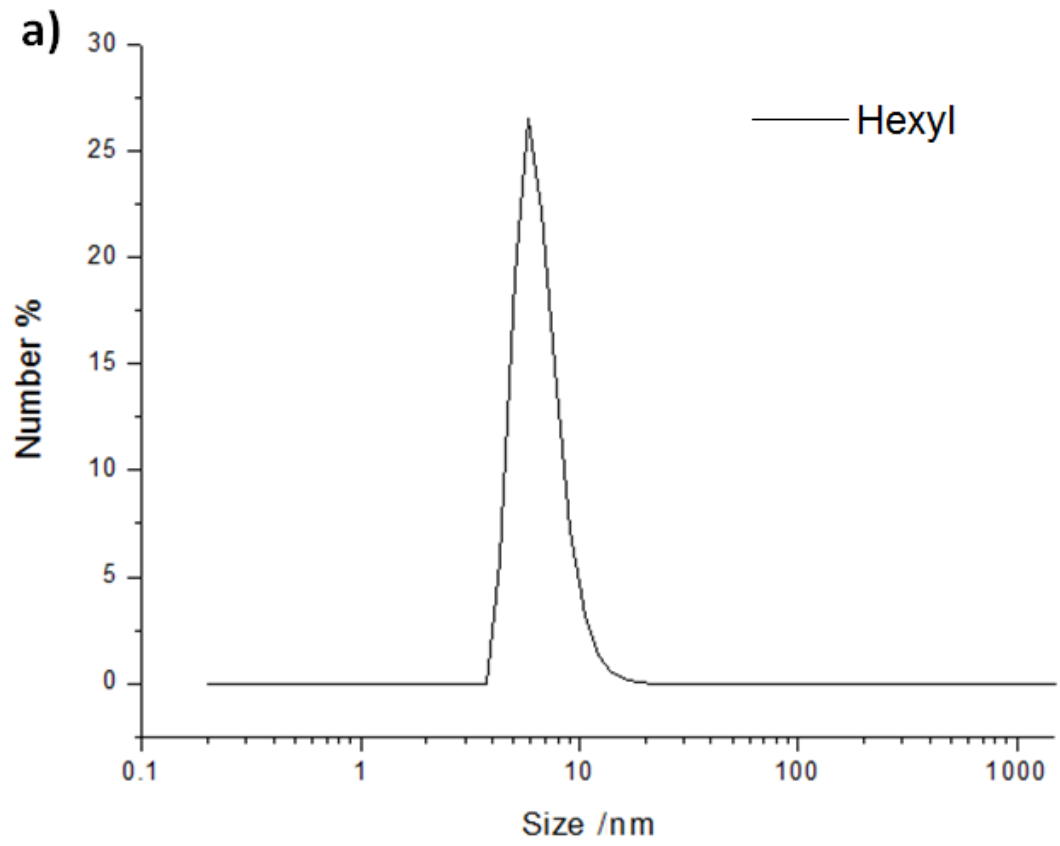
100 nm
HV=200.0kV
Direct Mag: 60000x
U.E.A Materials Science

Figure 6: TEM images of a) hexyl, b) octyl and c) dodecyl capped SiNPs produced via the methanol quenching reaction. Particles highlighted with red circles in a) and b) for clarity.

Table 2: Silicon core sizes and standard deviations for each of the three particle types produced by the MeOH quenched method.

Alkyl-SiNP	Average size /nm	Standard deviation /nm
Hexyl	5.6	1.4
Octyl	5.6	1.3
Dodecyl	5.8	1.4

DLS measurements revealed the hydrodynamic diameters of particles dispersed in organic solvent. Figure 7 a), b) and c) demonstrate the results of this analysis, giving mean diameters. The overall result of the DLS measurement is consistent with the TEM images, though DLS is not the most reliable technique for particles of such a small size. The percentage number of small particles indicates that these individual particles are dominant, as opposed to the presence of any large aggregates.



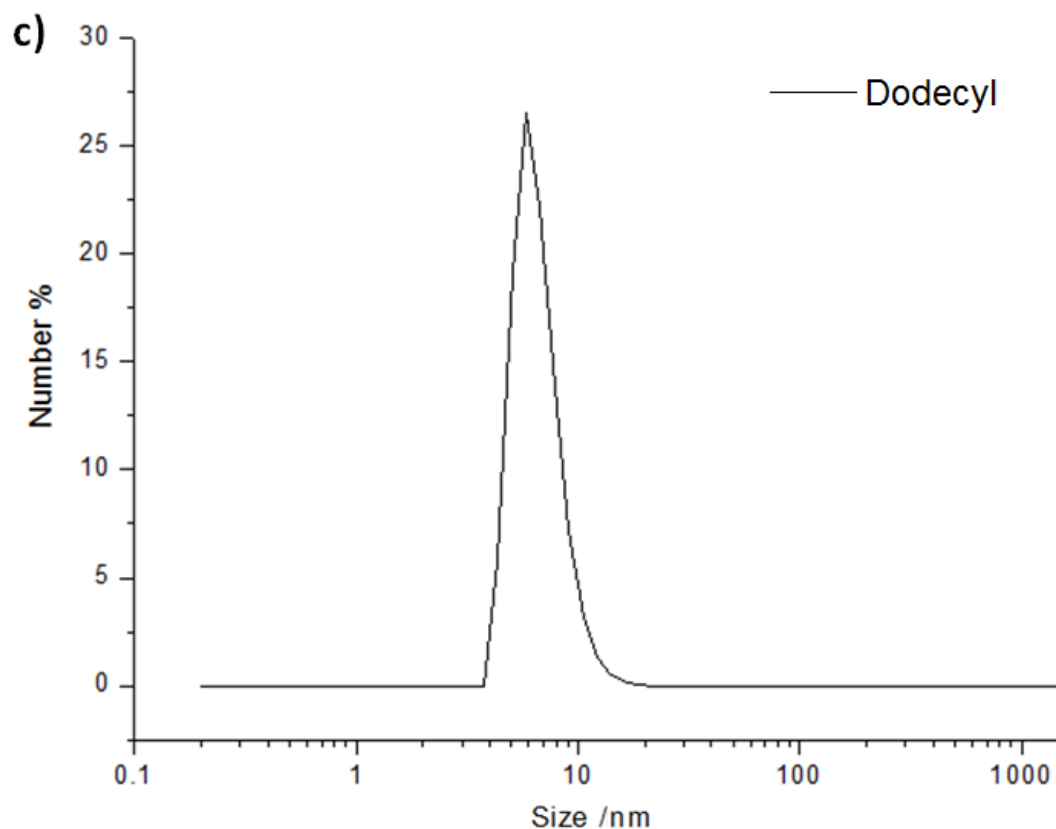


Figure 7: Hydrodynamic diameter expressed by number for alkyl-SiNPs a) hexyl, b) octyl and c) dodecyl produced by the MeOH quenched method.

3.2.3 PL and UV-Vis: optical properties

In order to first confirm the indirect bandgap properties of SiNPs, and to extrapolate an excitation wavelength, UV-Vis spectra were taken. UV-Vis spectra of hexyl-SiNPs are shown in Figure 8. This spectrum demonstrates a peak at 330 nm characteristic of the excitation wavelength of the sample, as an indirect band gap transition. UV-Vis spectra were used as a starting point in order to measure the optical properties of the particles produced, though given sample concentrations and timescales consistent data was difficult to produce. However, once the absorbance measured

was found to be reasonably consistent with the 330 nm figure a much more rigorous investigation was undertaken with PL spectroscopy. When further studied with PL spectroscopy, consistent strong excitation and emission peaks in the UV to blue region were resolved.

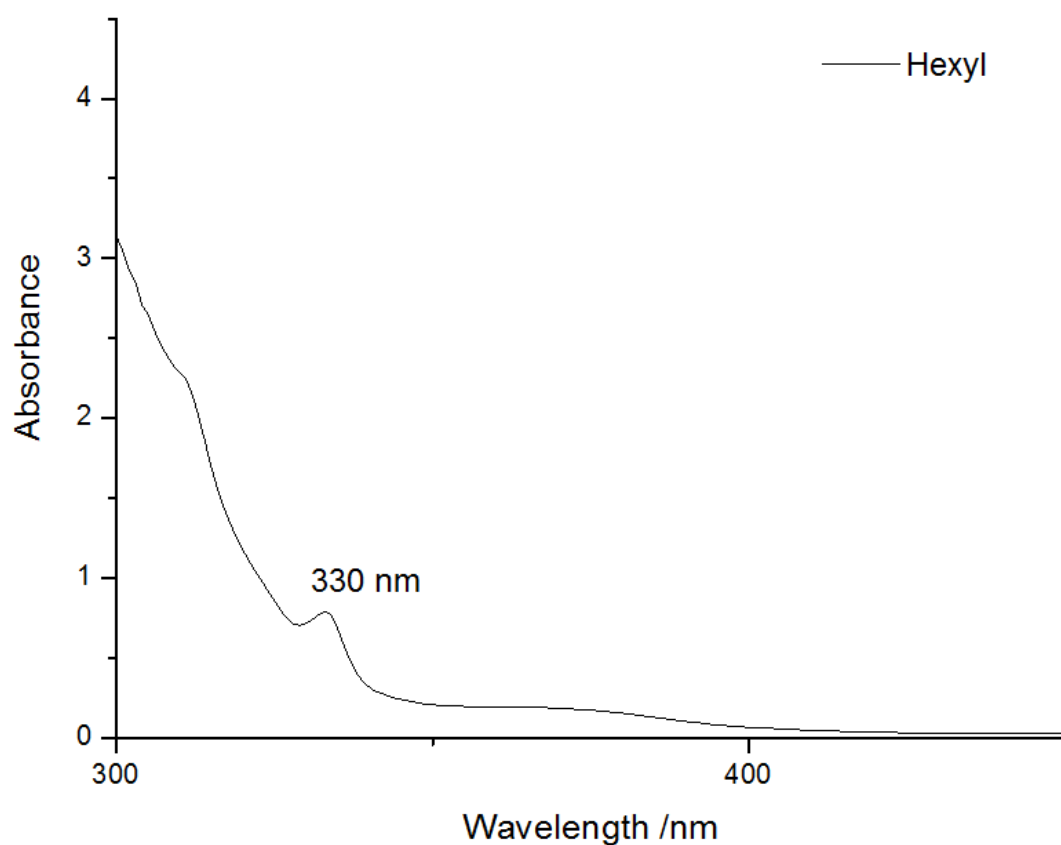
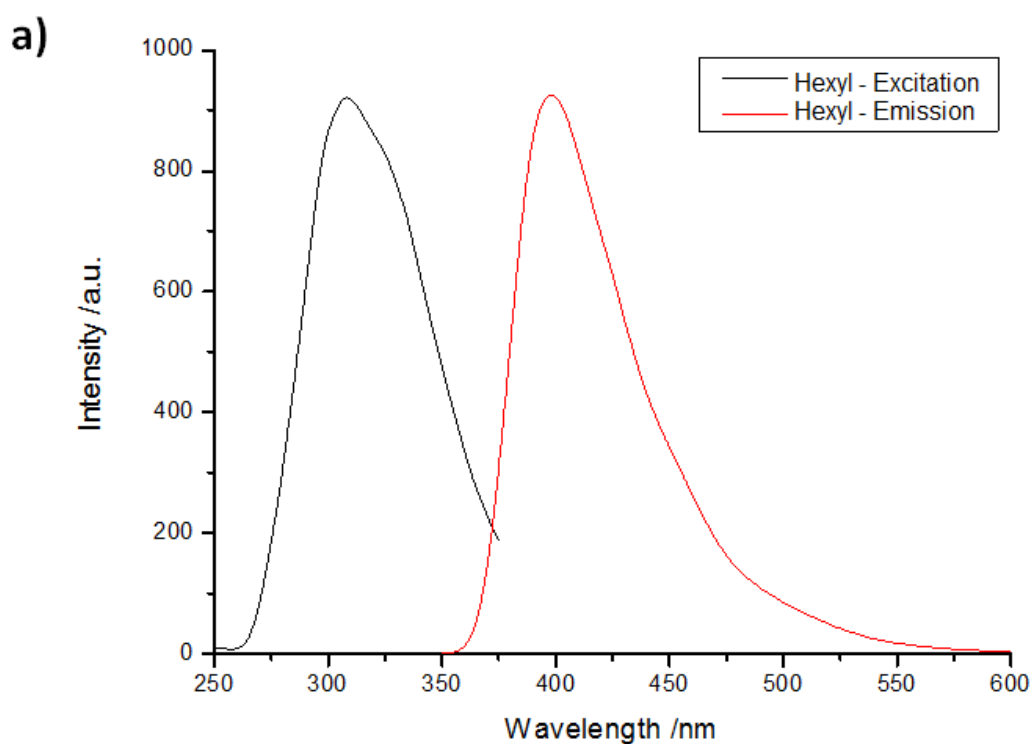
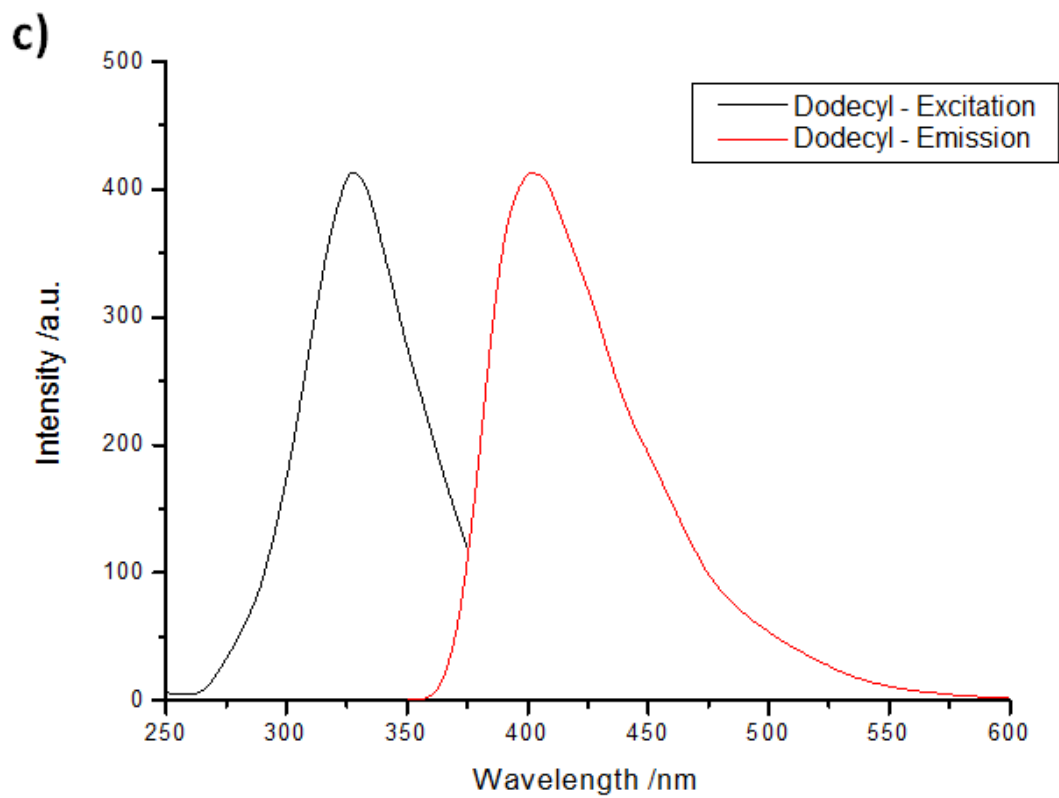
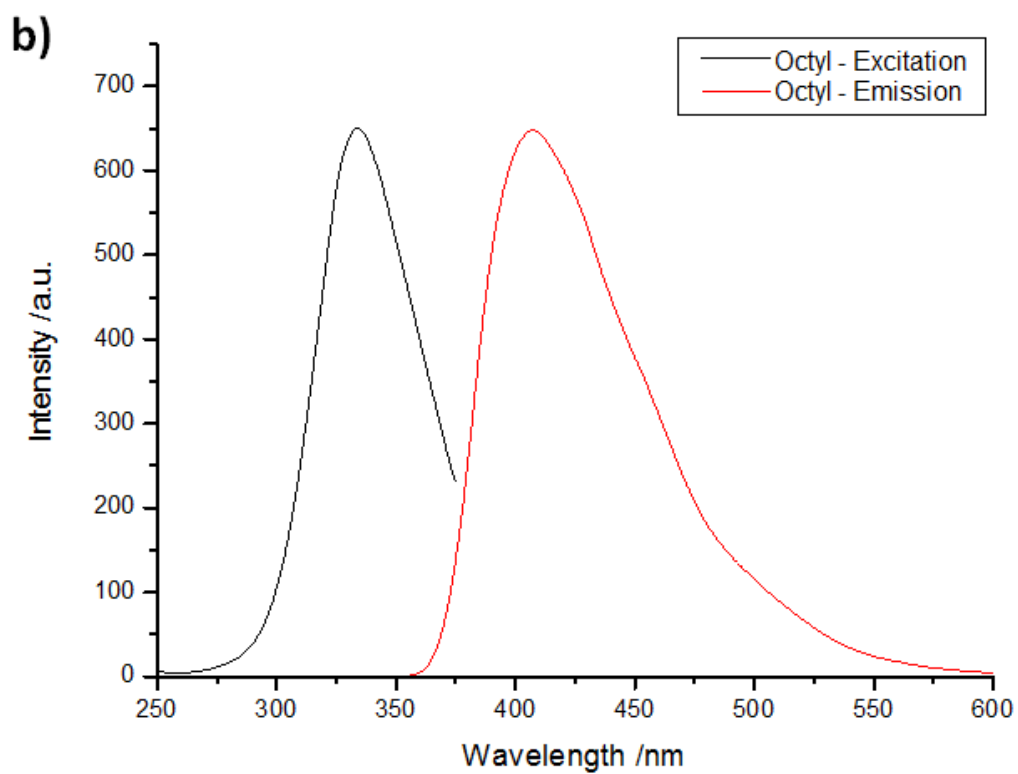


Figure 8: UV-Vis spectra for hexyl capped SiNPs produced from the methanol quenching mechanism, showing an indirect bandgap transition at a wavelength of 330 nm.

Figure 9 shows the photoluminescence properties of each of the different types of particles. Here the excitation and corresponding emission spectra are shown for each case. Overall, the spectra indicate a strong visible blue photoluminescence emission at wavelength 420 nm, when excited with UV radiation at wavelength 325 nm. In addition, Figure 9 d) shows a real colour image of a typical sample of Dodecyl-SiNPs suspended in hexane when subjected to a UV light source of wavelength 325 nm.





d)



Figure 9: PL emission and excitation spectra for a) Hexyl, b) octyl and c) dodecyl capped SiNPs produced via the methanol quenching option. d) shows a real colour image of a solution of dodecyl capped SiNPs suspended in Hexane when subjected to a 325 nm wavelength UV light source.

3.3 Summary

The consistent safe and easy production of a variety of alkyl passivated SiNPs with strong optical properties has been confirmed through TEM and DLS measurements from the this optimised one-pot synthesis method, and the quality of capping is very similar for all surfactants used, indicating that the method is easily adaptable for different functional groups, at least in the limited capacity explored here. The particle core sizes remained consistent across all three cases, indicating that with surfactants being modified in this way the particle structure is not notably affected.

In addition, the analysis of the particles optical properties indicated that they too were not notably affected by the change in capping layer, and results were consistent across all three cases, with strong blue PL emissions in each case.

However, limitations have been noted. The use of methanol clearly causes the presence of undesirable methoxy capping, as shown in the analysis of NMR and FTIR data. This is contrary to reports of Wang et al.²⁵ described above that the particles are susceptible to rapid oxidation when exposed to the atmosphere post synthesis. The capping of the particles with surfactant can never be made to be totally perfect, and thus in an attempt to rectify this alkoxy capping problem an alternative to the use of methanol to quench the excess reducing agent must be explored.

4 Quenching with CuCl₂: particle characterisation

4.1 Introduction

In chapter 4 the concerns outlined at the end of chapter 3 are addressed, namely the need to avoid methoxy capping of the product. This is achieved through use of CuCl₂ as detailed in chapter 2. Again, in the following analysis of the produced particles physical, chemical and optical properties for each of these three synthesised surface chemistries is explored using the analytical techniques detailed in chapter 2.

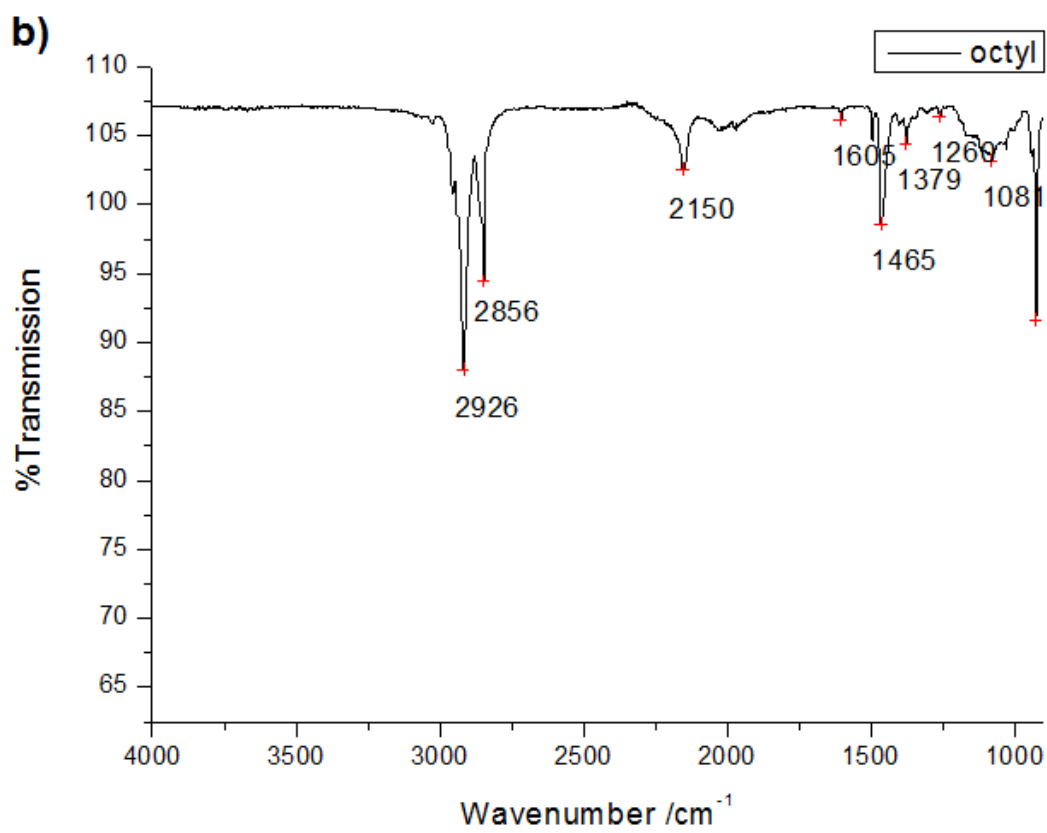
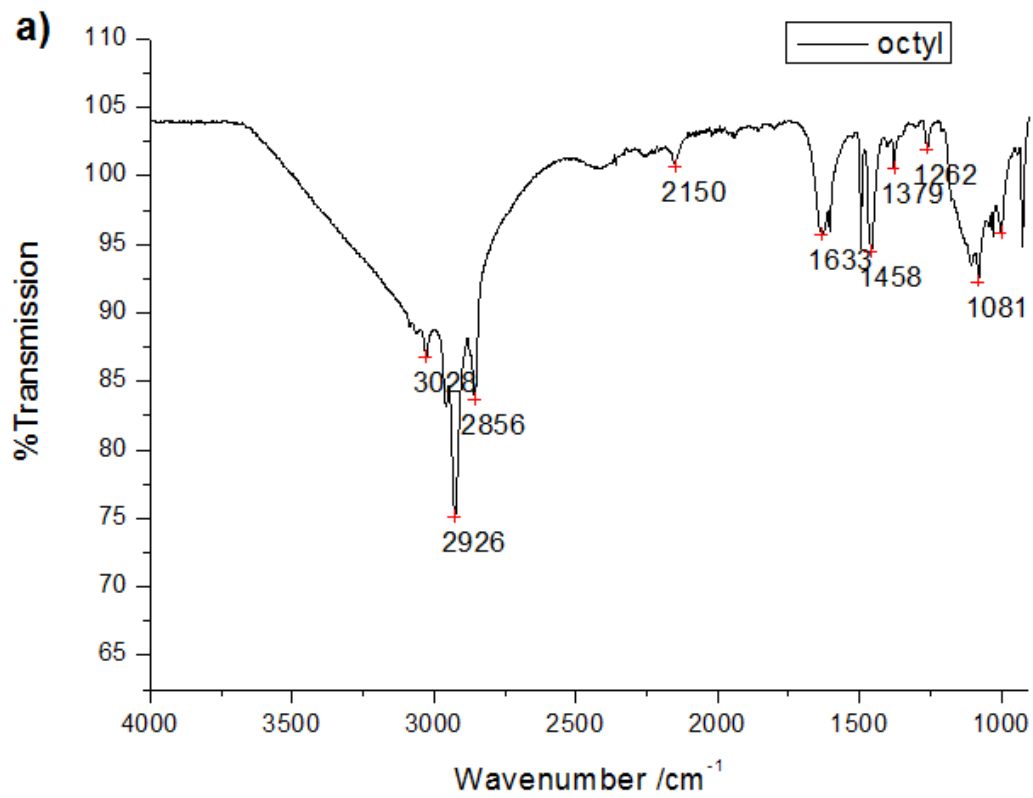
4.2 Alkyl-SiNP characteristics

4.2.1 FTIR and XPS: particle surface analysis

Distinct similarities between the FTIR spectra of chapter 3 and those shown in Figure 10 below indicates that alkyl functionalised silicon nanoparticles have been successfully synthesized. , with peaks at 1460 cm⁻¹, 2925 cm⁻¹ and 2852 cm⁻¹ to confirm the presence of Si-C and C-H bonds as discussed above. However, there are also some notable differences between the two methods. Firstly, and most importantly, the peaks primarily attributed to alkoxy functionality at 1084 cm⁻¹ and 1190 cm⁻¹ have vastly decreased in intensity. C-H bonds are now the most dominant bonds that can be seen in these spectra. There is a more dominant presence of Si-H bonds present as a result of this method, as evidenced by the peak as at 2150 cm⁻¹. However overall these bonds are still occurring in relatively negligible amounts as with the previous method. This increase is not entirely unexpected because any Si-H

bonds which were accessible to alkoxy groups in the previous method have not been attacked in this instance, and thus remain.

Secondly, the presence of a broad peak at 3000 to 3500 cm^{-1} in Figure 10 a) is characteristic of salt impurities which remained in the solution despite the usual filtering procedures. The addition of more stringent filtering procedures resulted in a clean sample, and indeed clean FTIR spectrum, see Figure 10 b) and c). However, the consequence of these additional procedures is a decreased yield (which has resulted in lower sample concentrations for measurement), since fewer particles are recovered in the final stages of filtration. Despite this, the yield is approximately 0.3 g and is easily scalable, which is still a large improvement on other competing methods such as electrochemical etching as discussed in chapter 1. Figure 10 c) shows an FTIR spectrum of the same sample 1 week after synthesis and remains unchanged. This indicates strong particle stability. Furthermore, there is no overall change in the amount of Si-H or Si-O observed in the sample. The small amount of Si-H present can therefore be said to be inaccessible and as such it can be further concluded that the samples in this capped state are not subject to any noticeable oxidation in air. These spectra have consistent scales and axis labels to facilitate easy comparison.



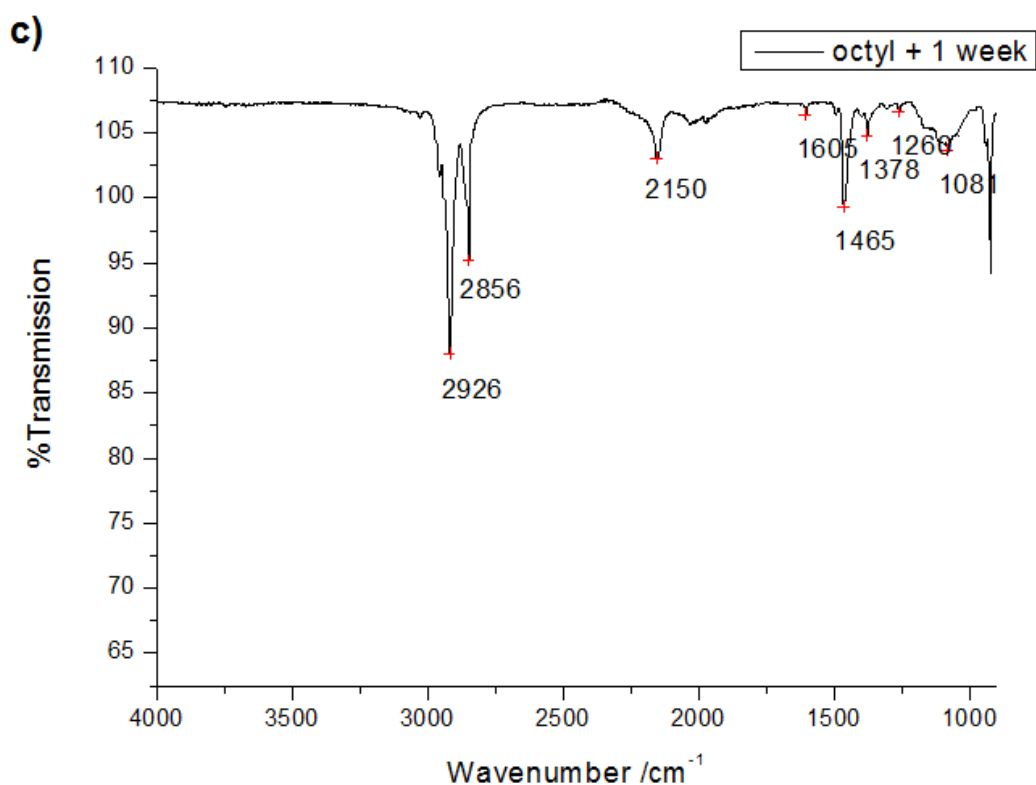
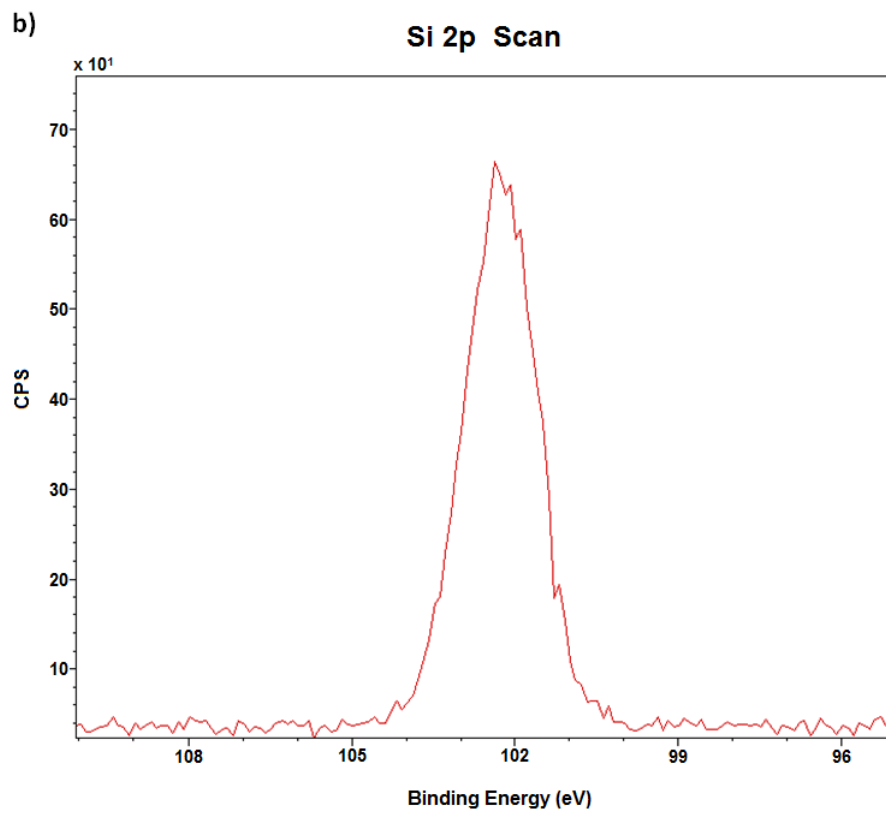
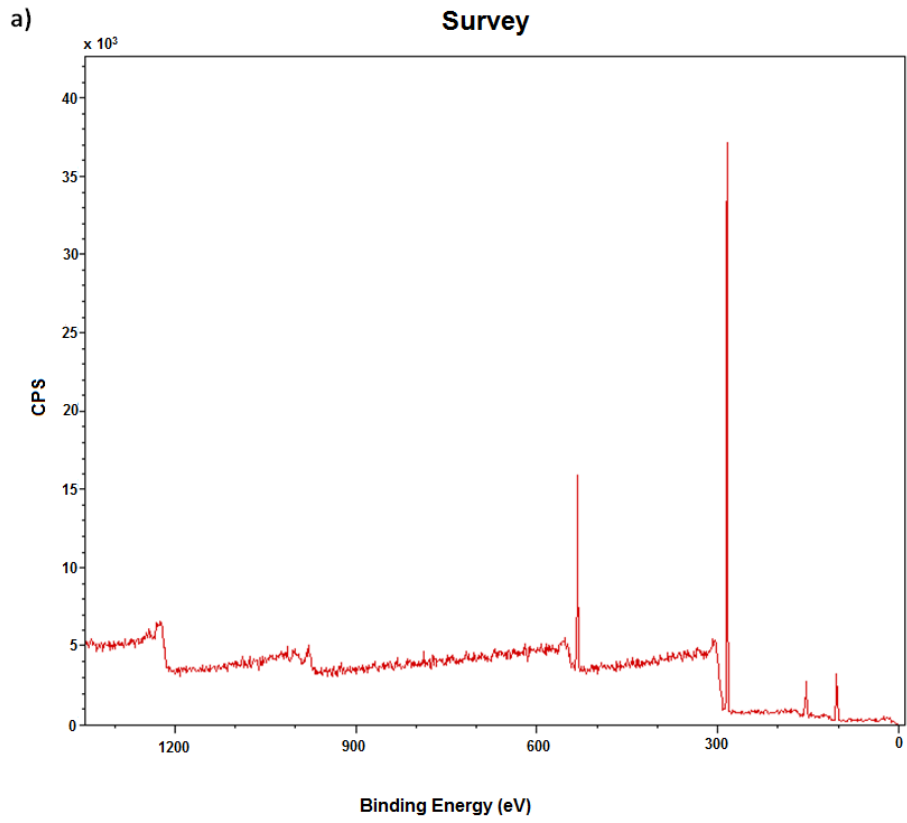
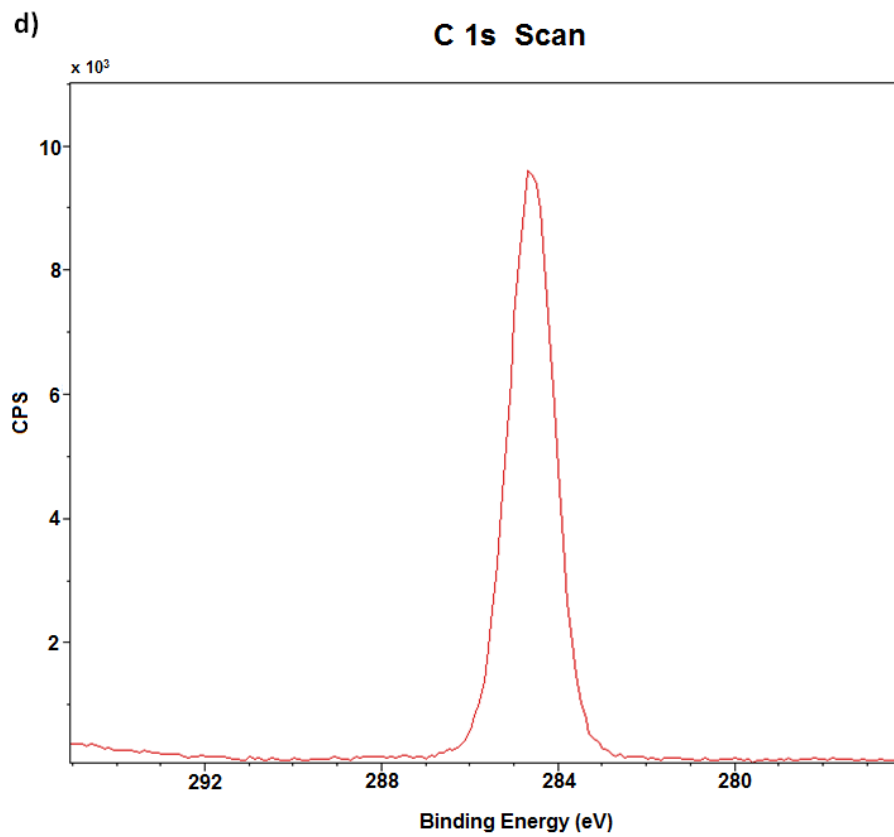
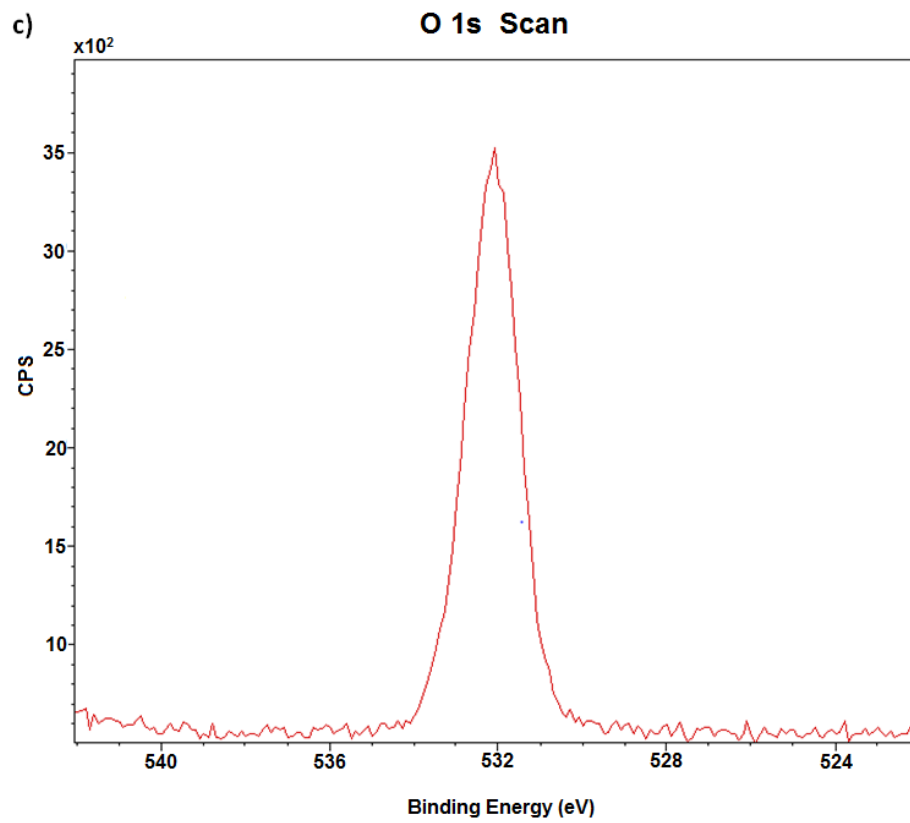


Figure 10: a) FTIR spectrum of a SiNP sample produced by this modified method but without any additional purification techniques showing broad salt peak at 3000 to 3500 cm^{-1} . b) FTIR spectrum of the same sample once additional purification techniques have been used. c) FTIR spectrum of the same sample + 1 week showing stability.

In order to further explore the surface functionality XPS was used on a dodecyl-SiNP sample prepared via this method in order to show surface elemental analysis. Figure 11 shows an abundance of silicon, oxygen and carbon in the elemental analysis as would be expected for a layer of SiNPs. Oxygen is expected for particles of this nature due to the oxidative effect of the x-rays interacting with the sample, and so it

is not a good indicator of normal surface oxidation. For clarity, narrow band scans of the region where nitrogen and copper peaks may be seen, (Figure 11 e) and f) respectively) and show only background fluctuations. This confirms the purity of the final product.





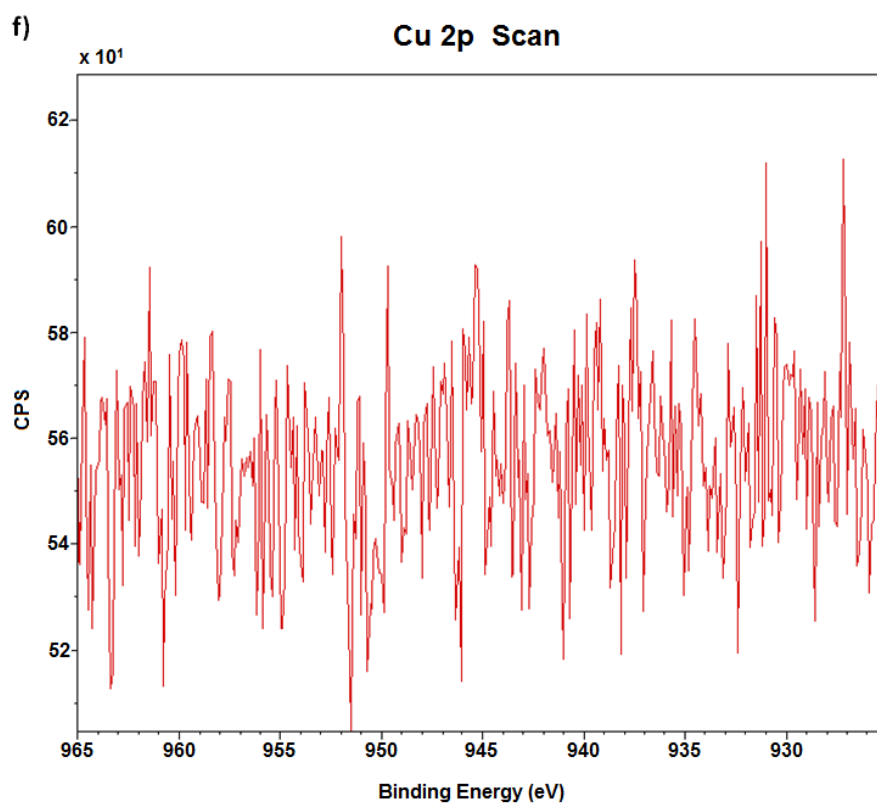
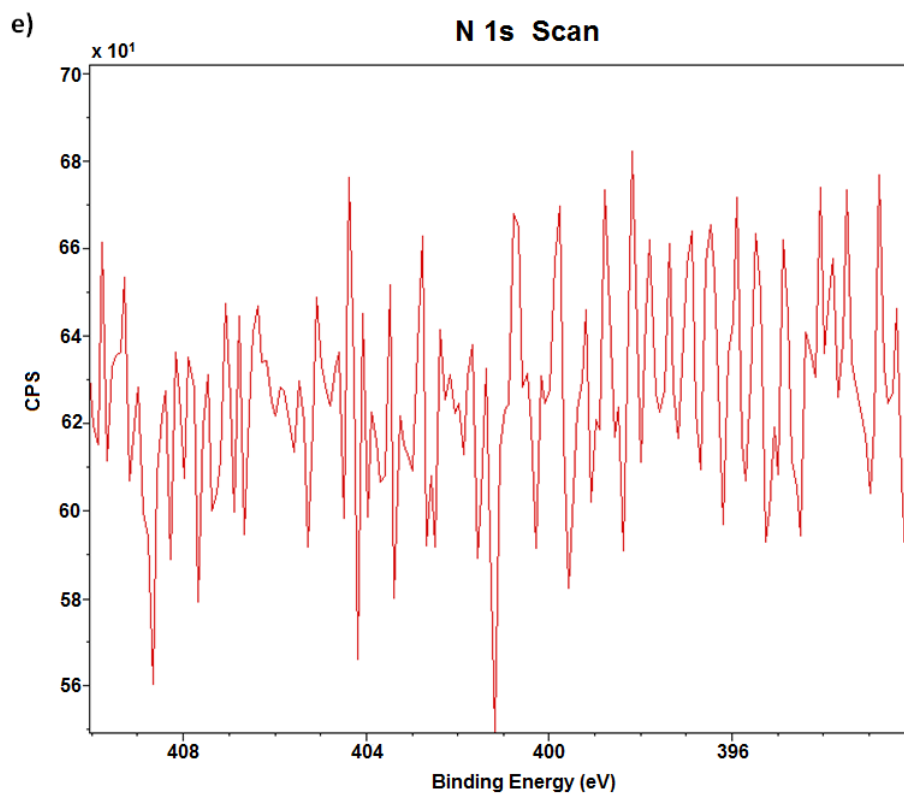
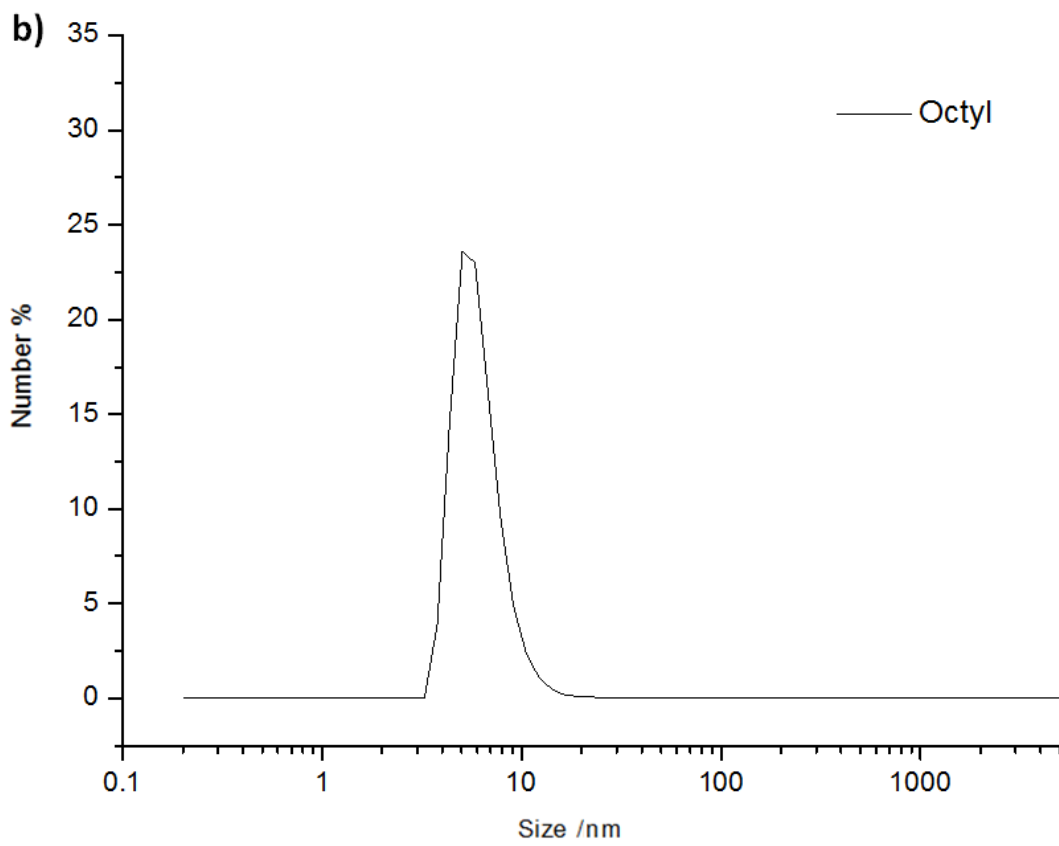
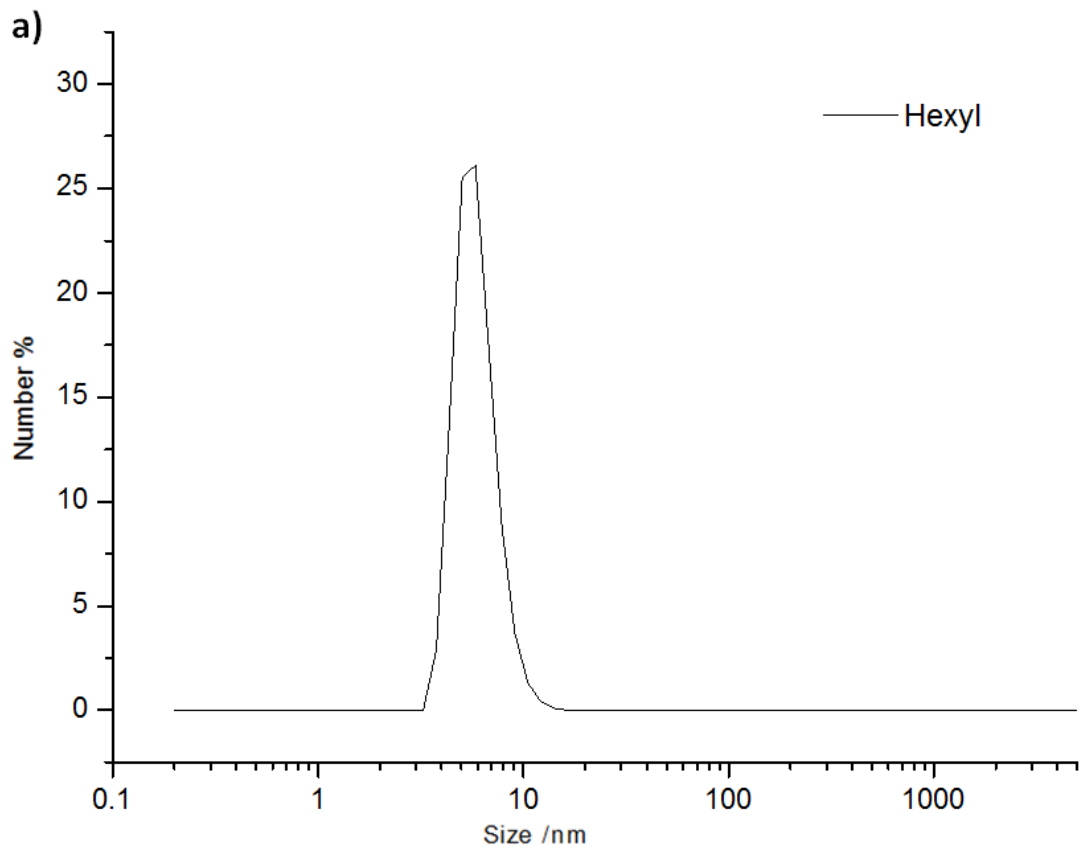


Figure 11: XPS surface elemental analysis of a sample of dodecyl-SiNPs. a) Survey spectrum of all elements, b) silicon peak (Si2p), c) oxygen peak (O1s), d) carbon peak (C1s), e) no peak, background only in nitrogen (N1) region, f) no peak, background only in copper (Cu2p) region.

4.2.2 TEM, STEM and DLS: particle size and structure

Imaging and sizing results are not dissimilar to those shown in chapter 3, though the lower yields observed due to the incorporation of additional filtration steps has resulted in more difficulty acquiring data and particle images in particular.

DLS hydrodynamic diameters of particles dispersed in organic solvent. Figure 12 a), b) and c) demonstrate the results of this analysis, giving mean diameters. The overall result of the DLS measurement is consistent with the TEM images given the size discrepancy expected. Again, the percentage number of small particles indicates that the individual particles are dominant, as opposed to the presence of any large aggregates.



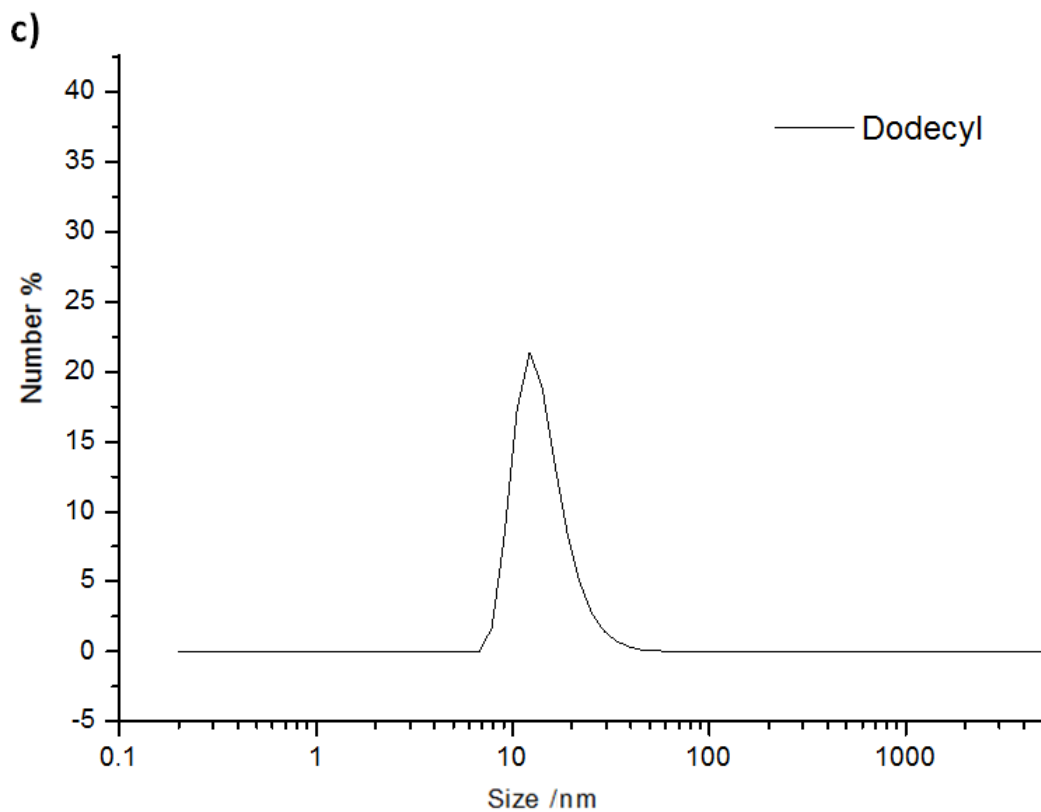
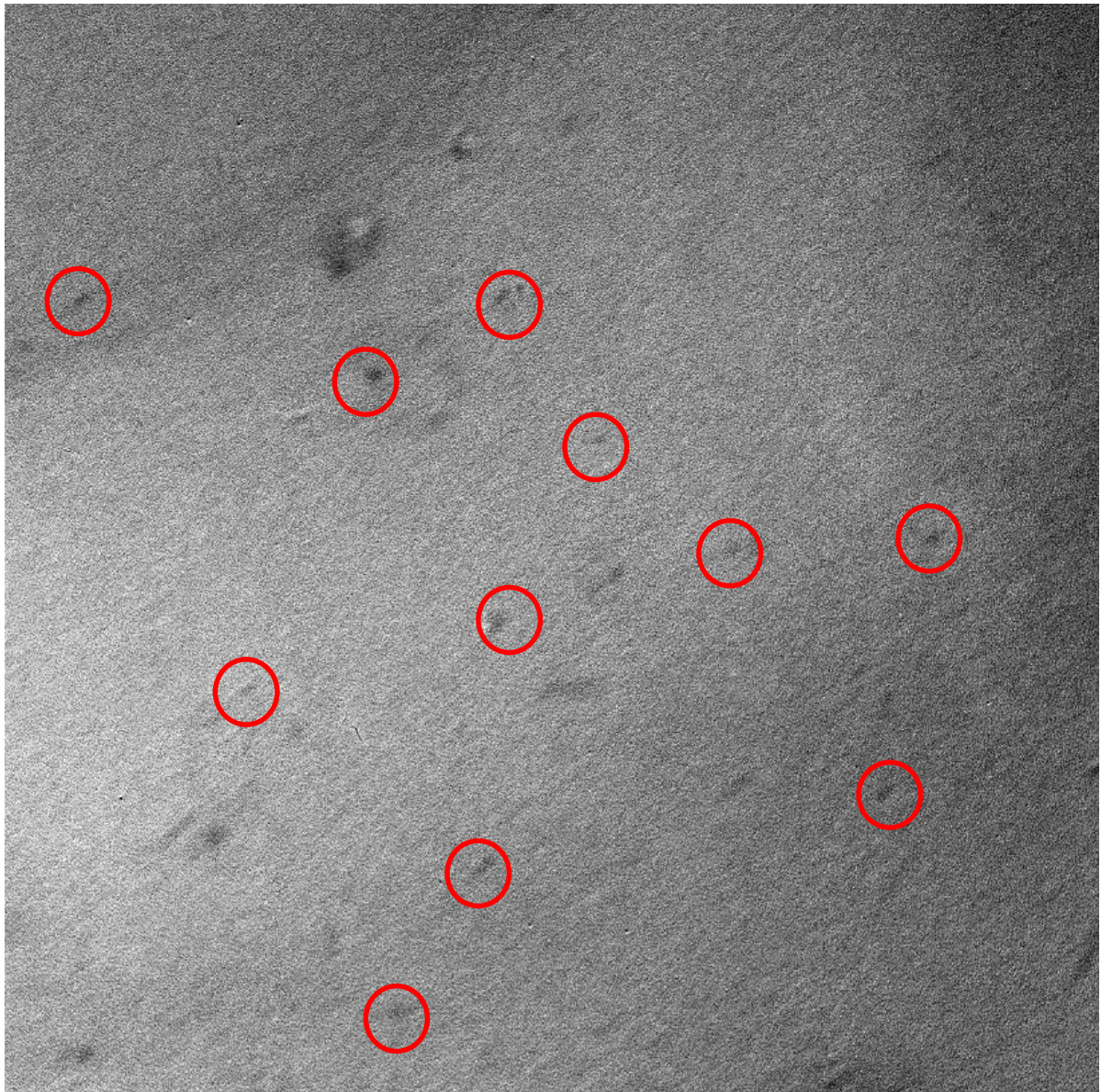


Figure 12: Hydrodynamic diameter expressed by number for alkyl-SiNPs a) hexyl, b) octyl and c) dodecyl produced by the CuCl_2 quenched method.

TEM images of the particles produced by this method are displayed in Figure 13, again the observed size distribution is consistent with those detailed in chapter 3 and the change of quenching agent has had no adverse effect on particle morphology. Table 3 indicates the measured sizes and monodispersity.

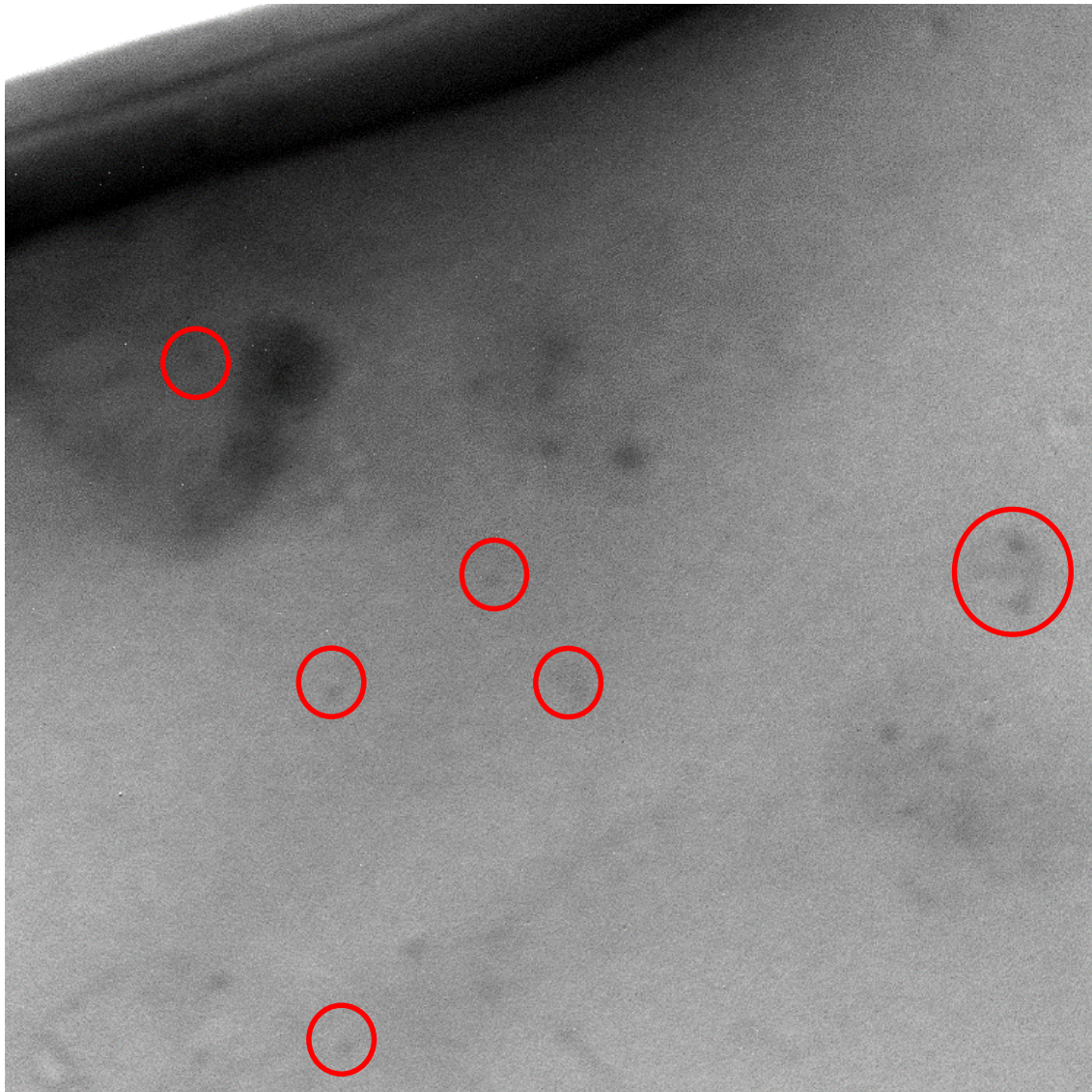
a)



N11.11.tif
TEM Mode: Imaging

100 nm
HV=200.0kV
Direct Mag: 50000x
U.E.A Materials Science

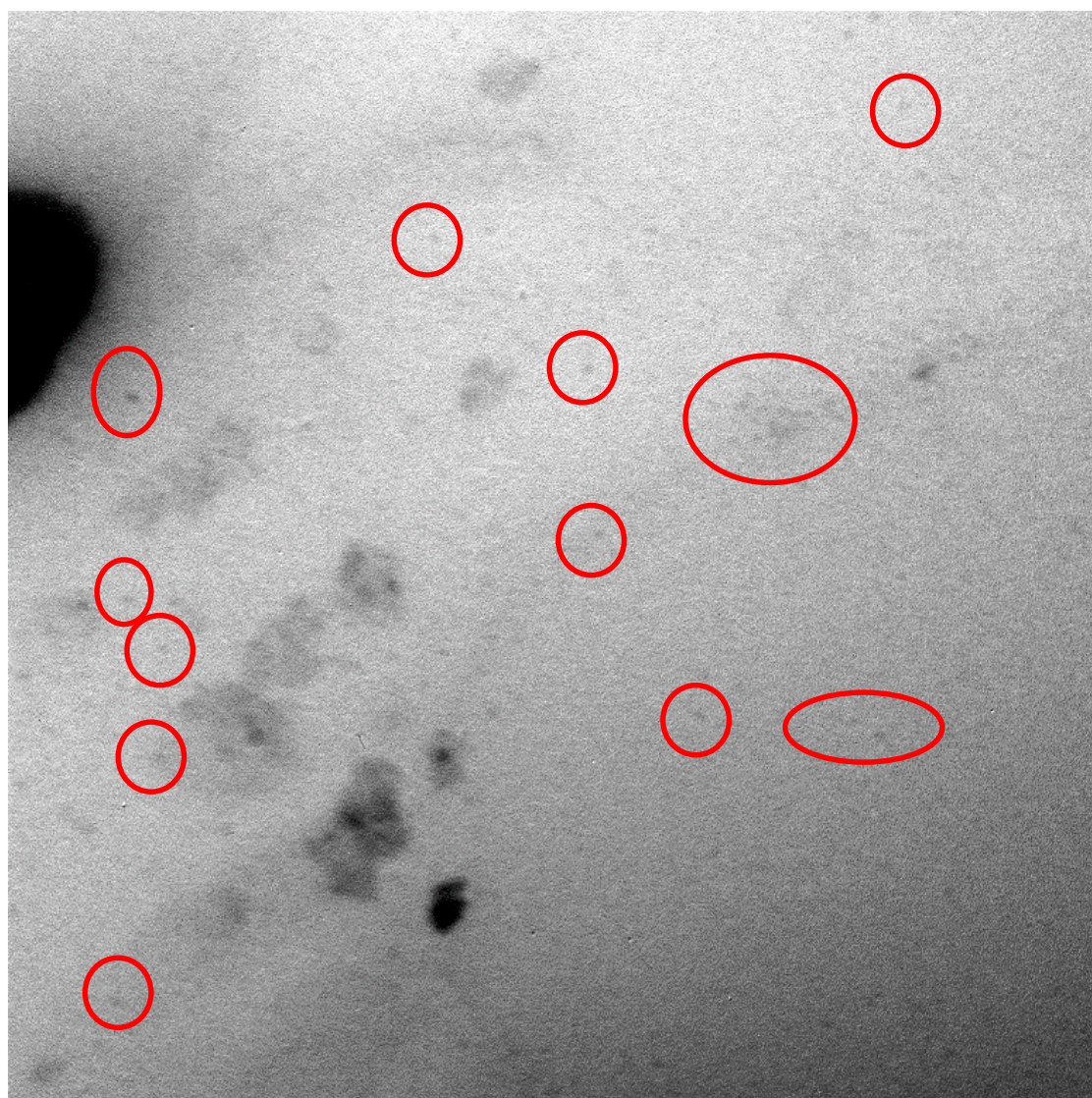
b)



N11.14.tif
TEM Mode: Imaging

100 nm
HV=200.0kV
Direct Mag: 60000x
U.E.A Materials Science

c)



N11.20.tif
TEM Mode: Imaging

100 nm
HV=200.0kV
Direct Mag: 40000x
U.E.A Materials Science

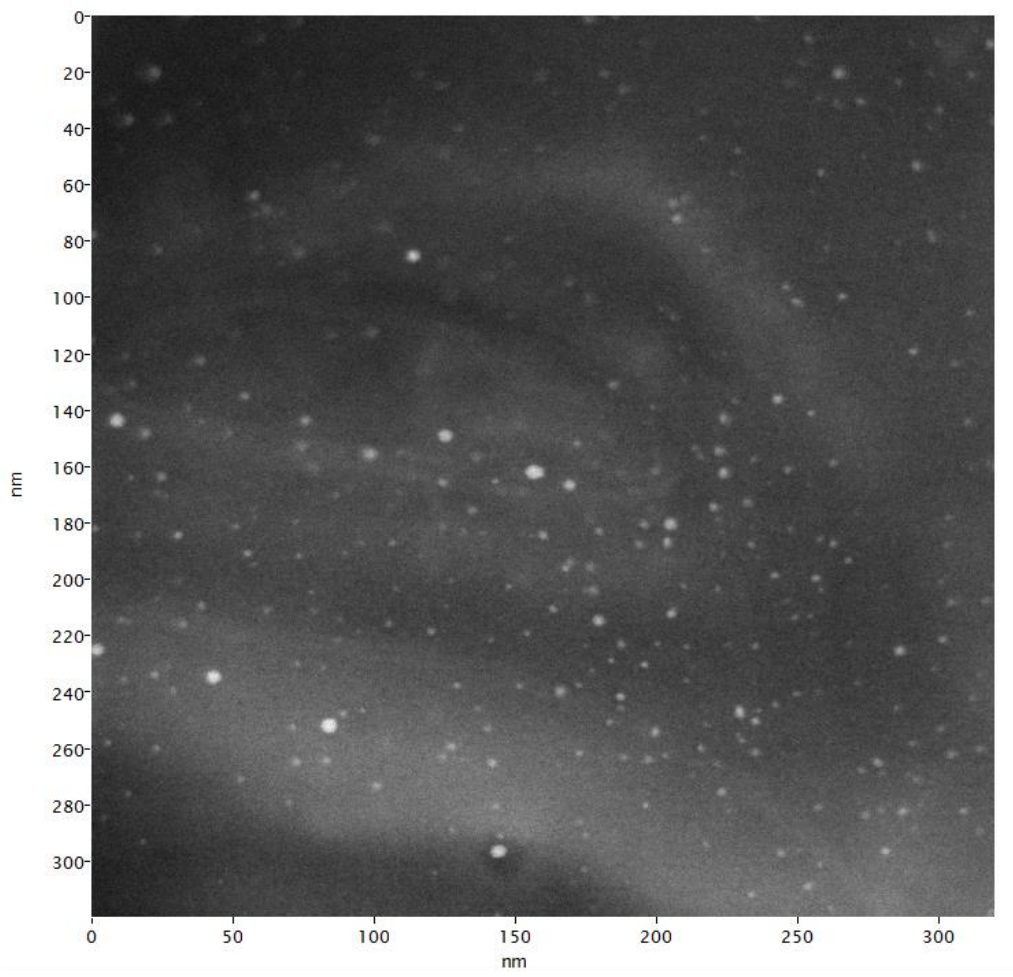
Figure 13: TEM images of a) hexyl, b) octyl and c) dodecyl capped SiNPs produced via the CuCl_2 quenching reaction. Some particles are highlighted with red circles for clarity.

Table 3: Silicon core sizes and standard deviations for each of the three particle types produced by the CuCl₂ quenched method.

Alkyl-SiNP	Average size /nm	Standard deviation /nm
Hexyl	5.6	1.6
Octyl	5.7	1.8
Dodecyl	5.7	1.4

In addition to TEM images, STEM images were taken of hexyl-SiNPs produced by this method. The silicon core of the particles produced by both methods detailed above are shown to be fundamentally the same, and ultimately show similar physical properties. Due to the particles small size and poor contrast it is a notable challenge to make suitable sizing measurements or to produce images of the particles as discussed previously. Figure 14 a) shows an STEM Z-contrast image of hexyl capped SiNPs with a high resolution image of a single particle in Figure 14 b). This high resolution image allows for the core to be seen up close, including a detailed view of the lattice structure. The measured lattice fringe spacing in the crystalline particle shown is 0.31 nm, corresponding to the (111) interplanar spacing of the diamond cubic structure of silicon.

a)



b)

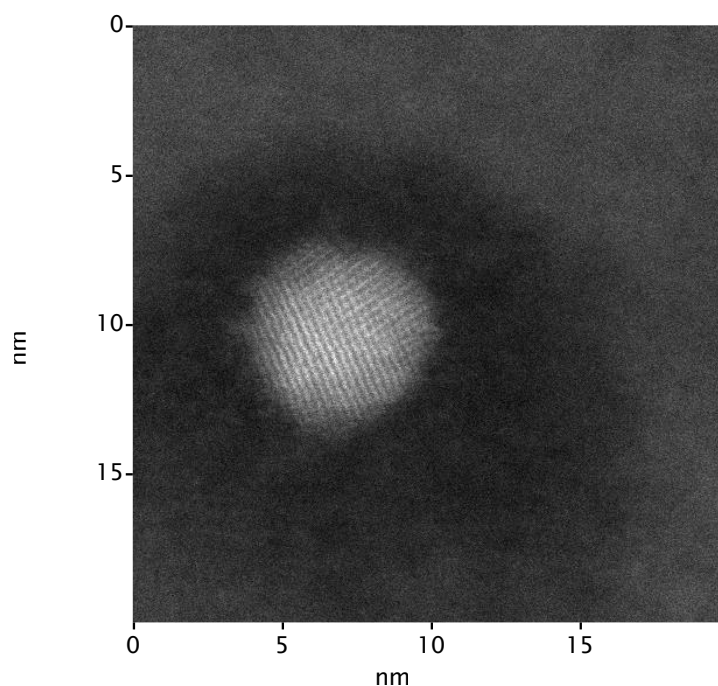
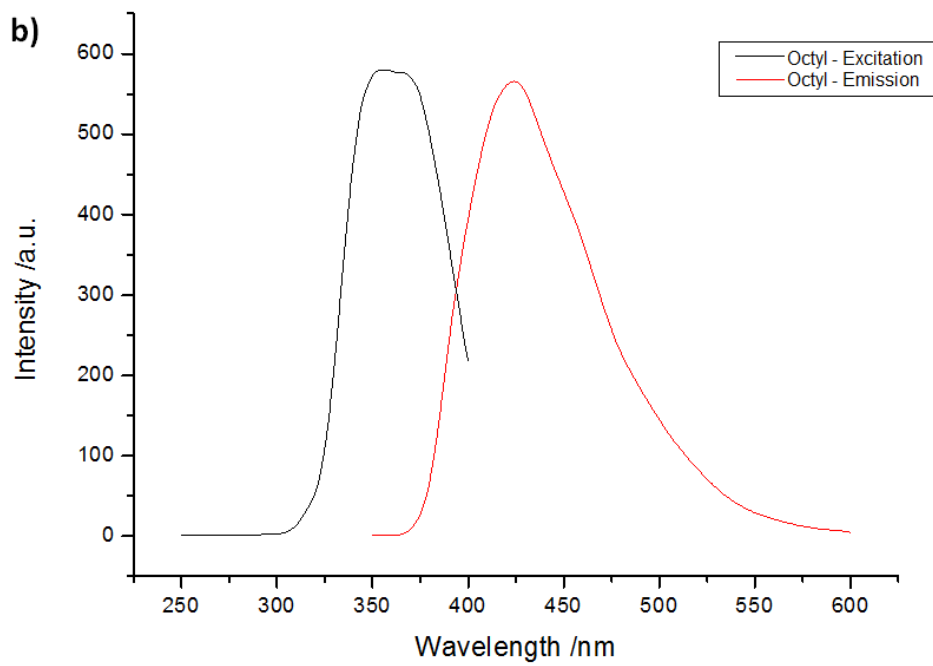
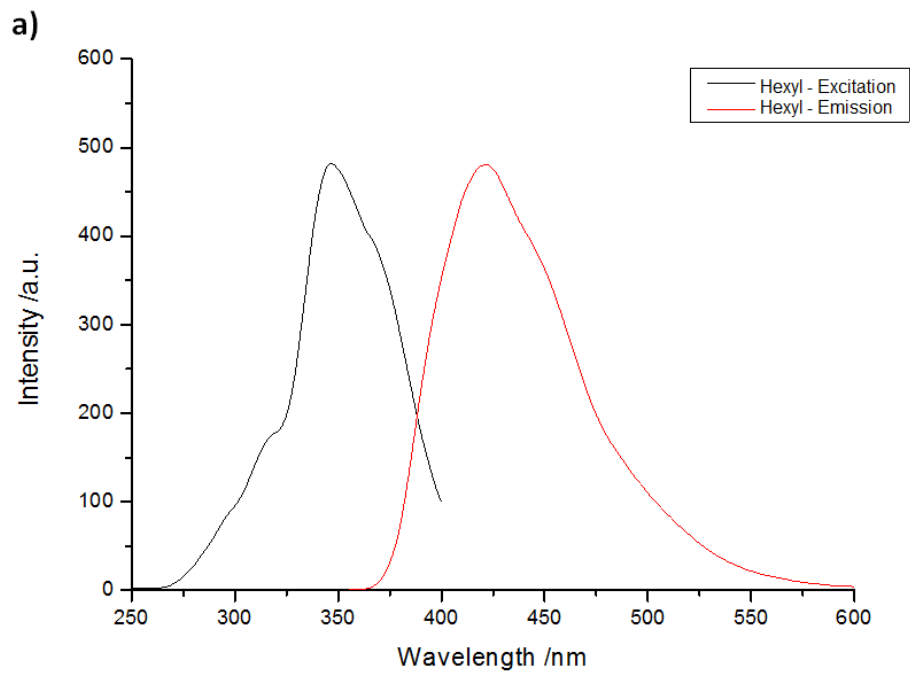
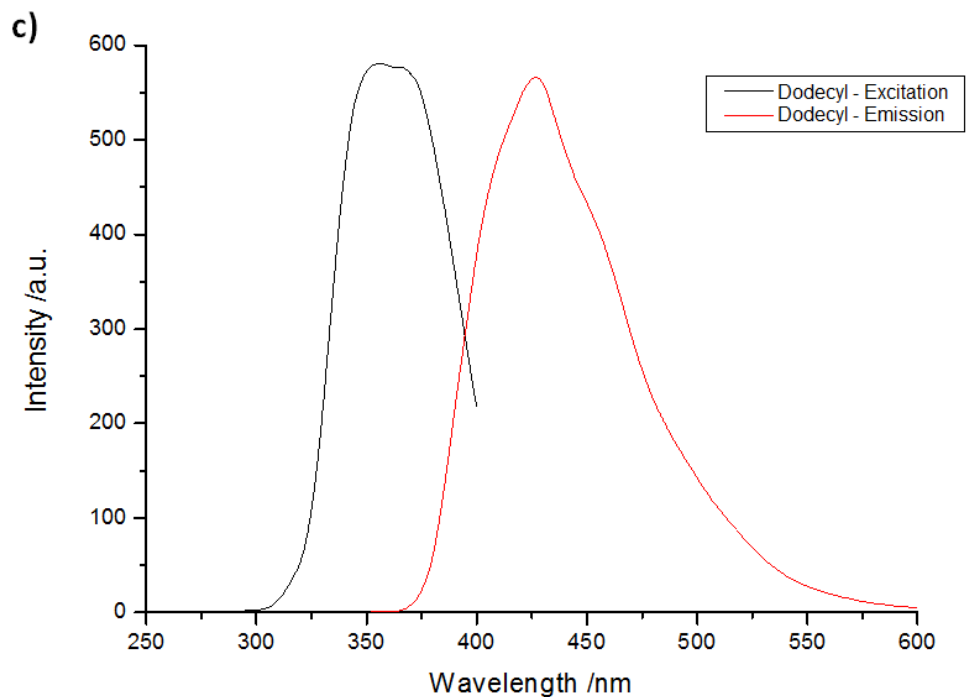


Figure 14: STEM images of hexyl-SiNPs. a) standard image of sea of particles, b) high resolution close up image of a single particle, demonstrating 0.31 nm crystalline silicon lattice fringe spacing.

4.2.3 PL and UV-Vis: optical properties

The optical properties of the samples not exposed to alkoxy ligands by virtue of the use of CuCl_2 to quench the reducing agent are comparable to those of those that are quenched with an alcohol. As can be seen in the PL spectra, Figure 15, these particles also show a strong UV excitation centred at 325 nm and blue emission peak centred at 420 nm. In addition, Figure 15 d) shows a real colour image of a typical sample of Dodecyl-SiNPs.





d)



Figure 15: PL emission and excitation spectra for a) hexyl, b) octyl and c) dodecyl capped SiNPs produced via the CuCl_2 quenching option. d) shows a real colour image of a solution of dodecyl capped SiNPs suspended in Hexane when subjected to a 325 nm wavelength UV light source.

4.3 Summary

The results of this approach are largely very similar to those from chapter 3. The particles have similar morphology and size distribution, and the surface chemistry is improved now that the alkoxy capping problem has been eliminated.

The incorporation of the XPS analysis technique for these samples also indicates that the purification procedures put in place have successfully eliminated the presence of copper in the final product.

The additional filtration required to purify the final product in this method results in more of the product being lost, and this a lower effective yield. However, this yield is still greater than the commonly used top-down counterpart described in chapter 1.

Optically the particles are again similar to those from chapter 3, once again qualifying the overall lack of interference with the product, as well as again indicating that changes in particle surface oxidation does not appear to have any noticeable impact on the particles optical properties.

5 Conclusions and future work

Alkyl passivated silicon nanoparticles were produced via a cheap, fast, safe and high yielding one-pot, inverse micelle based method that is easily scalable. This methods limitations included the contamination of the particles surface chemistry with alkoxy groups, and thus the work finds additional novelty in a revised method by virtue of the use of anhydrous copper (II) chloride to quench excess reducing agent present in the system. This addresses the methods previously identified primary flaw. The reaction conditions were also optimised in order to minimise the existence of 'uncapped' Si-H surface termination. The resultant particles are low oxide, highly functionalised and stably passivated, with a strong blue photoluminescence. The copper (II) chloride quenched particles demonstrate a lack of Si-O-C surface functionality as expected. These features are clearly demonstrated via a plethora of structural, elemental and luminescence spectroscopic techniques. However, the products of this reaction are contaminated with heavy metals and by-products which require additional purification steps in order to remove; this results in a lower overall yield than the earlier method.

Of particular note, surface elemental analysis through XPS has shown that there are no nitrogen containing compounds present in the resulting product, whilst PL spectroscopy shows no presence of any orange luminescence. This result is contrary to that of a recent publication by Dasog et al.³⁹ and suggests that a more complex system must be at play. Nitrogen containing surfactants cannot be solely responsible for quenching orange luminescence in SiNPs. Equally, a decrease in Si-O bonds and a maintained strong blue photoluminescence may suggest that oxygen in the surface

chemistry is not the main factor determining blue wavelength emission. This data prompts further investigation into the reasoning behind SiNP optical behaviour, reasoning which remains elusive. It may also be wise to consider approaching the luminescence properties from a theoretical modelling approach in the future, in order to gain a better understanding of the system. If the optical properties of these particles are to be investigated further a reasonable next step would also be to look into the quantum yield of the particles, which was not reported as part of this work simply due to time constraints.

In addition, the particles produced are found to be in a gel/oil state, even when fully dried. In the literature the phase of the product produced by any of the numerous different synthesis methods often remains unreported. With the phase of the produced particles here being quite unusual, comparison with the product of other synthesis methods would prove to be an interesting study. Another area of investigation would be to study the product and model the interactions that are causing it to exist in such a fashion. The particles produced, despite their surface groups, appeared to change negligibly in terms of size and morphology. This may be different if different or more complex groups of surfactants are used.

Although capping silicon nanoparticles with simple alkyl chains has potential applications, it is really just the beginning. This method has the potential to be used in many synthesis types, making innumerable surface conditions facile to produce. A next step would be to adapt this method to accommodate different ligands which might open the doors to various new applications. For example hydrophilic particles, with phosphate, sulphate or nitrate ligands, would allow particles that can be

introduced into biological systems to be quickly, safely and easily produced. Such particles might be used in bio-fluorescence imaging and would be a step into new territory for this work.

6 References and publications

6.1 References

1: Alivisatos A. P., Semiconductor clusters, nanocrystals, and quantum dots. *Science*, 1996, 271, 933 - 937.

2: Ahire J., Wang Q., Coxon P., Malhotra G., Brydson R., Chen R., Chao Y., Highly luminescent and nontoxic amine-capped nanoparticles from porous silicon: synthesis and their use in bioimaging, *ACS applied materials & interfaces*, 2012, 4, 3285 - 3292.

3: Ashby S. P., Garcia-Cañadas J., Min G., Chao Y., Measurement of Thermoelectric Properties of Phenylacetylene-Capped Silicon Nanoparticles and their potential in fabrication of Thermoelectric Materials, *Journal of Electronic Materials*, 2013, 47, 1495 - 1498.

4: Bangal M., Ashtaputre S., Marathe S., Ethiraj A., Hebalkar N., Gosavi S., Urban J., Kulkarni, S., Semiconductor nanoparticles. *Hyperfine Interactions*, 2005, 160, 81 - 94.

5: Pickett N.L., O'Brien P., Synthesis of semiconductor nanoparticles using single-molecular precursors. *The Chemical Record*, 2001, 1, 467 - 479.

6: Einevoll G. T., Confinement of excitons in quantum dots. *Physical Review B*, 1992, 45, 3410 - 3417.

7: Henglein A., Small-particle research: Physicochemical properties of extremely small colloidal metal and semiconductor particles. *Chemical Reviews*, 1989, 89, 1861 - 1873.

- 8: Hagfeldt A., Graetzel M., Light-induced redox reactions in nanocrystalline systems. *Chemical Reviews*, 1995, 95, 49 - 68.
- 9: Fendler J. H., Meldrum F. C., The colloid chemical approach to nanostructured materials. *Advanced Materials*, 1995, 7, 607 - 632.
- 10: Alivisatos A. P., Perspectives on the physical chemistry of semiconductor nanocrystals. *The Journal of Physical Chemistry*, 1996, 100, 13226 - 13239.
- 11: Brus L. E., Electron electron and electron-hole interactions in small semiconductor crystallites - the size dependence of the lowest excited electronic state. *Journal of Chemical Physics*, 1984, 80, 4403 - 4409.
- 12: Nirmal M., Brus, L., Luminescence photophysics in semiconductor nanocrystals. *Accounts of Chemical Research*, 1999, 32, 407 - 414.
- 13: Zanella M., Falgui A., Kudera S., Manna L., Casula M. F., Parak W. J., Growth of colloidal nanoparticles of group II-VI and IV-VI semiconductors on top of magnetic iron-platinum nanocrystals, *Journal of Materials Chemistry*, 2008, 18, 4311 - 4317.
- 14: Delerue C., Allan G., Lannoo M., Optical band gap of si nanoclusters. *Journal of Luminescence*, 1998, 80, 65 - 73.
- 15: Belomoin G., Rogozhina E., Therrien J., Braun P. V., Abuhassan L., Nayfeh M. H., Wagner L., Mitas L., Effects of surface termination on the band gap of ultrabright si-29 nanoparticles: Experiments and computational models. *Physical Review B*, 2002, 65.

- 16: Heath J. R., A liquid-solution-phase synthesis of crystalline silicon. *Science*, 1992, 258, 1131 - 1133.
- 17: Canham L. T., Silicon quantum wire array fabrication by electrochemical and chemical dissolution of wafers. *Applied Physics Letters*, 1990, 57, 1046 - 1048.
- 18: Heinrich J. L., Curtis C. L., Credo G. M., Kavanagh K. L., Sailor M. J., Luminescent colloidal silicon suspensions from porous silicon. *Science*, 1992, 255, 66 - 68.
- 19: Belomoin G., Therrien J., Smith A., Rao S., Twesten R., Chaieb S., Nayfeh M. H., Wagner L., Mitas L., Observation of a magic discrete family of ultrabright silicon nanoparticles. *Applied Physics Letters*, 2002, 80, 841 - 843.
- 20: Lie L. H., Duerdin M., Tuite E. M., Houlton A., Horrocks B. R., Preparation and characterisation of luminescent alkylated-silicon quantum dots. *Journal of Electroanalytical Chemistry*, 2002, 538, 183 - 190.
- 21: Chao Y., Krishnamurthy S., Montalti M., Lie L. H., Houlton A., Horrocks B. R., Kjeldgaard L., Dhanak V. R., Hunt M. R. C., Siller L., Reactions and luminescence in passivated silicon nanocrystallites induced by vacuum ultraviolet and soft-x-ray photons. *Journal of Applied Physics*, 2005, 98.
- 22: Bley R. A., Kauzlarich S. M., A low-temperature solution phase route for the synthesis of silicon nanoclusters. *Journal of the American Chemical Society*, 1996, 118, 12461 - 12462.
- 23: Wilcoxon J. P., Samara G. A., Provencio P. N., Optical and electronic properties of silicon nanoclusters synthesized in inverse micelles. *Physical Review B*, 1999, 60, 2704.

- 24: Tilley R. D., Warner J. H., Yamamoto K., Matsui I., Fujimori H., Micro-emulsion synthesis of monodisperse surface stabilized silicon nanocrystals. *Chemical Communications*, 2005, 1833 - 1835.
- 25: Wang J., Sun S., Peng F., Sun L., Efficient one-pot synthesis of highly photoluminescent alkyl-functionalised silicon nanocrystals, *Chemical Communications*, 2011, 4941 - 4943.
- 26: Stewart M. P., Buriak J. M., New approaches toward the formation of silicon-carbon bonds on porous silicon. *Comments on Inorganic Chemistry*, 2002, 23, 179 - 203.
- 27: Li X. G., He Y. Q., Swihart M. T., Surface functionalization of silicon nanoparticles produced by laser-driven pyrolysis of silane followed by hf-hno3 etching. *Langmuir*, 2004, 20, 4720 - 4727.
- 28: Sato S., Swihart M. T., Propionic-acid- : Synthesis and optical characterization. *Chemistry of Materials*, 2006, 18, 4083 - 4088.
- 29: Salata O., Applications of nanoparticles in biology and medicine. *Journal of Nanobiotechnology*, 2004, 2, 3.
- 30: Ghaderi S., Ramesh B., Seifalian A. M., Fluorescence nanoparticles "quantum dots" as drug delivery system and their toxicity: A review. *Journal of Drug Targetting*, 2011, 19, 475 - 486.
- 31: Sharifi S., Behzadi S., Laurent S., Forrest M. L., Stroeve P., Mahmoudi M., Toxicity of nanomaterials. *Chemical Society Reviews*, 2012, 41, 2323 - 2343.

- 32: Lewinski N., Colvin V., Drezek R., Cytotoxicity of nanoparticles. *Small*, 2008, 4, 26 - 49.
- 33: Warner J. H., Hoshino A., Yamamoto K., Tilley R. D., Water-soluble photoluminescent silicon quantum dots. *Angewandte Chemie International Edition*, 2005, 44, 4550 - 4554.
- 34: Van Vlerken L. E., Amiji M. M., Multi-functional polymeric nanoparticles for tumour-targeted drug delivery. *Expert Opinion on Drug Delivery*, 2006, 3, 205 - 216.
- 35: Snyder G. J., Small Thermoelectric Generators, *The electrochemical society Interface*, 2008, 3, 54 - 56.
- 36: Hochbaum A. I., Chen R., Delgado R. D., Liang W., Garnett E. C., Najarian M., Majumdar M., Yang P., Enhanced thermoelectric performance of rough silicon nanowires, *Nature*, 2008, 451, 163 - 167.
- 37: Venkatasubramanian R., Siivola E., Colpitts T., O'Quinn B., Thin-film thermoelectric devices with high room-temperature figures of merit, *Nature*, 2001, 413, 597 - 602.
- 38: Rier C., Schierning G., Wiggers H., Schmechel R., Jäger D., Photovoltaic Devices from Silicon Nanoparticles, *MRS Proceedings*, 2010, 1230, 39.
- 39: Dasog M., Yang Z., Regil S., Tilley R.D., Veinot J. G. C., Chemical insight into the origin of red and blue photoluminescence arising from freestanding silicon nanocrystals, *ACS Nano*, 2013, 7, 2676 – 2685.

6.2 Publications

Ashby, S., **Thomas, J.**, Coxon, P., Bilton, M., Brydson, R., Pennycook, T., Chao, Y., The effect of alkyl chain length on the level of capping of silicon nanoparticles produced by a one-pot synthesis route based on the chemical reduction of micelle. *Journal of Nanoparticle Research*, 2013, 15:1425.

Wenchao Z., Baoqing, Y., Ruiqi S., Jiahai Y., **Thomas, J.**, Chao, Y., Significantly Enhanced Energy Output from 3D Ordered Macroporous Structured Fe₂O₃/Al Nanothermite Film. *ACS Applied Materials and Interfaces*, 2013, 5 (2), p. 239-242.

Zhang, W., Xu, B., Wang, L., Wang, X., **Thomas, J.**, Chao, Y., Synthesis of nickel picrate energetic film in a 3D ordered silicon microchannel plate through an in situ chemical reaction. *Journal of Materials Science*, 2013, 48 (23), p. 8302-8307